Carbazole-Embedded Cyclodimer adopting Helical Conformation and Metal-ion Sensing

Athira Naniyil, Arun Kumar, Aathira Edwin, and Sabapathi Gokulnath*

Indian Institute of Science Education and Research Thiruvananthapuram, Kerala-695551, India.

1. General Information

The reagents and materials for the synthesis were used as obtained from Sigma -Aldrich chemical suppliers. All solvents were purified and dried by standard methods prior to use. Thin-layer chromatography (TLC) was carried out on aluminum sheets coated with silica gel 60 F254 (Merck 5554). Silica gel column chromatography was performed on Wakogel C-230 - 400 mesh. Alumina column chromatography was performed on Active alumina (basic). Recrystallized samples of porphyrinoids were utilized for all the spectroscopic measurements. The High-resolution mass spectra (HRMS) were recorded on Q Exactive TM-Bench top-LC-HRMS mass spectrometer. ^{1}H NMR (500) and ^{13}C NMR (125 MHz) spectra were recorded on BRUKER Avance 500 MHz spectrometer, and chemical shifts were reported as the delta scale in ppm relative to CH_2Cl_2 as an internal reference for ^{1}H (5.32 ppm) and for ^{13}C (53.84 ppm). The optical absorption spectra were recorded on a Shimadzu (Model UV-3600) spectrophotometer. Concentrations of the solutions are *ca*. to be 1 x 10^{-6} M. Single crystal X-ray data were collected on a Bruker KAPPA APEXII diffractometer in omega and phi scan mode, MoKα = 0.71073 Å at liquid nitrogen temperature.

Theoretical Calculations: All calculations were carried out using the Gaussian 16 program package.[S1] Calculations were performed by the density functional theory (DFT) method with restricted B3LYP (Becke's three-parameter hybrid exchange functional and the Lee-Yang-Parr correlation functional)[S2] level, employing a basis sets 6-31G(d). Vertical electronic excitations were based on B3LYP-optimized geometries using the time-dependent density functional theory (TD-DFT) formalism.[S3] The nucleus-independent chemical shift (NICS (0)) values were determined at the mean position of the core atoms of the optimized structures by the B3LYP/6-31G(d) method. Anisotropy of the current-induced density (ACID) plots were obtained by employing the continuous set of gauge transformations method to calculate the current densities, and the results were plotted by using POVRAY.

X-ray Crystal Structure Analysis: Single crystal was grown by slow vapour diffusion of methanol into a THF solution of **1**. Single crystal was mounted at 140 K on a three-circle Bruker SMART APEX CCD area detector system under a Mo-Kα (λ = 0.71073 Å) graphite monochromatic X-ray beam. The structures were solved by direct methods and least-square refinement on F2 for **1** by using SHELXS-97. All non-hydrogen atoms were refined anisotropically. The hydrogen atoms were included in the structure factor calculation by using a riding model. The solvent molecule that could not be identified or modified in **1** was fixed

and eventually squeezed using PLATON. The crystallographic parameters, data collection, and structure refinement of **1** is summarized in Table S6-1.

2. Synthetic Procedures and Compound Data

Synthesis of 1,8-Di(-1*H*-pyrrole)-3,6-di-*tert*-butyl)-9*H*-carbazole **3** was accomplished by our previously reported procedure.[S4]

Synthesis of 1: To a 250 mL two-neck round bottom flask containing compound **3** (100 mg, 0.244 mmol) and [2,2′-bithiophene]-5,5′-diylbis-(mesitylmethanol) **4** (112.8 mg, 0.244 mmol), 100 ml dry CH_2Cl_2 was added and stirred under Ar atmosphere under the dark. Trifluoroacetic acid (TFA) (8.57 µL, 0.122 mmol) was added and the mixture was allowed to stir for 1 h. To the reaction mixture, 2,3-dichloro-5,6-dicyano-*p*-benzoquinone (DDQ) (110 mg, 0.488 mmol) was added and allowed to stir for a further 10 min at room temperature. The entire reaction mixture was filtered through a pad of basic alumina and eluted with CH_2Cl_2 until the eluent was no longer dark. The resulting crude mixture was concentrated by rotary evaporator to give a purple solid. The crude solid was purified by alumina column chromatography. The purple fraction eluted with 10% CH_2Cl_2/hexane provided **1** as a purple solid in 12% (24 mg) yield. ^{1}H NMR (500 MHz, CD_2Cl_2) δ 11.68, 9.17, 8.39, 8.37, 8.33, 7.90, 7.38, 7.28, 7.00, 6.97, 6.85, 6.82, 6.73, 6.57, 6.36, 2.37, 2.31, 2.23, 2.06, 2.00, 1.67, 1.54. HRMS (ESI) *m/z*: $[M]^+$; calcd for: $C_{112}H_{107}N_6S_4$: 1663.7440; Found 1663.7432, error in ppm = 0.48.

Mass Spectral analysis of 1:

Mass spectrometric studies were conducted on macrocycle **1** upon the addition of Ag^+ and Hg^{2+} ions. The solutions were prepared in methanol. In the case of mercury bound species, the ESI-MS spectrum was recorded which showed a peak corresponding to the dimetallated complex, where each Hg^{2+} ion is coordinated to one acetate group and to a carbazole nitrogen through deprotonation. ESI-MS: *m/z* = 2182.6980 ($[M]^+$; *calcd* for $C_{116}H_{110}Hg_2N_6O_4S_4$ = 2182.6884). Upon addition of silver ions to macrocycle **1**, mass corresponding to the hydrogen adduct of the bis-metalated complex was observed. HR-MS (HESI): *m/z* = 1875.5399 ($[M+H]^+$; *calcd* for $C_{112}H_{105}Ag_2N_6S_4$ = 1875.5385). HESI = Heated Electrospray Ionization.

3. High-Resolution APCI-TOF Mass Spectra

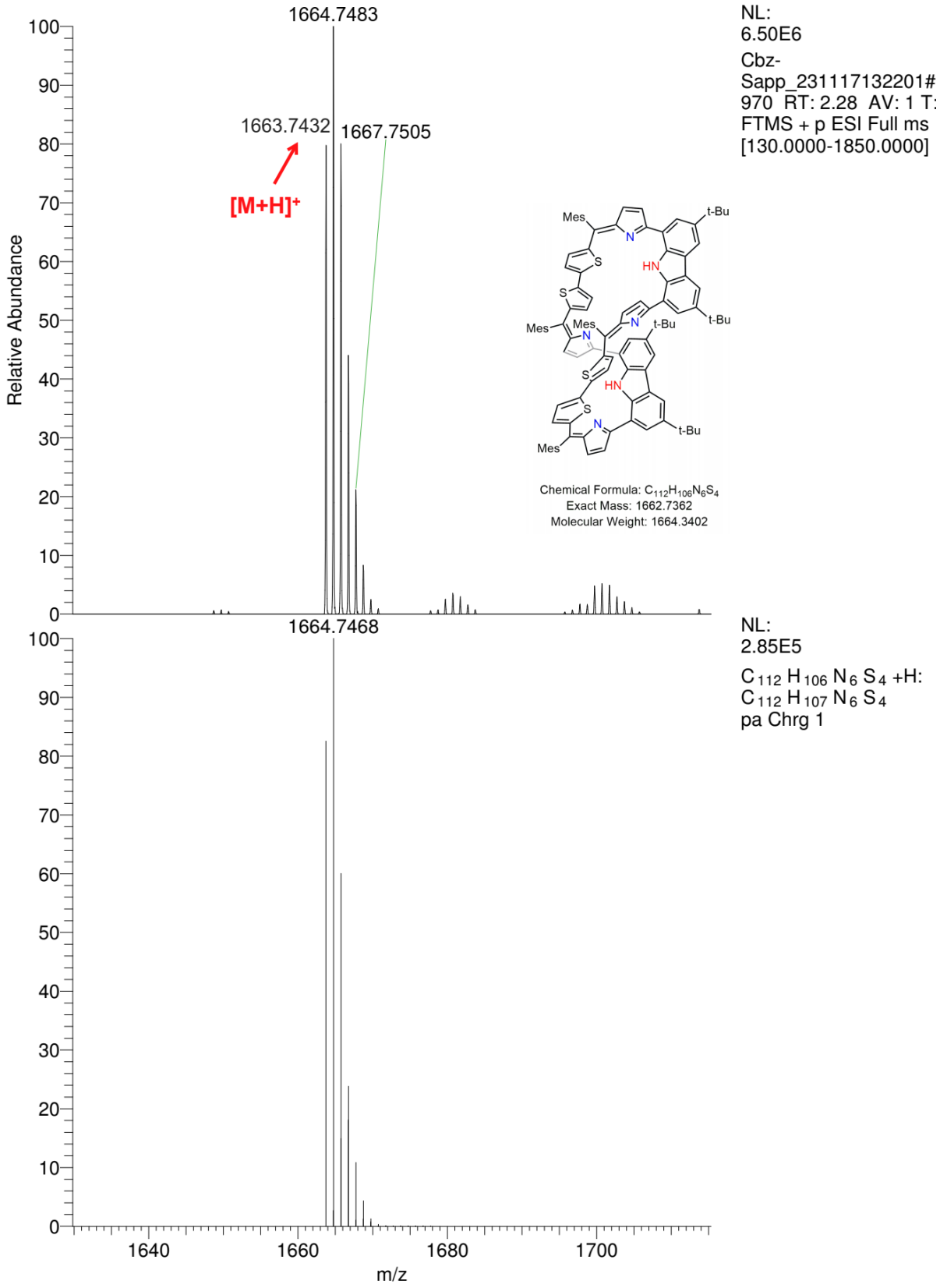

Figure S1. High-Resolution Mass Spectrum of **1** (top) and simulated spectrum (bottom)

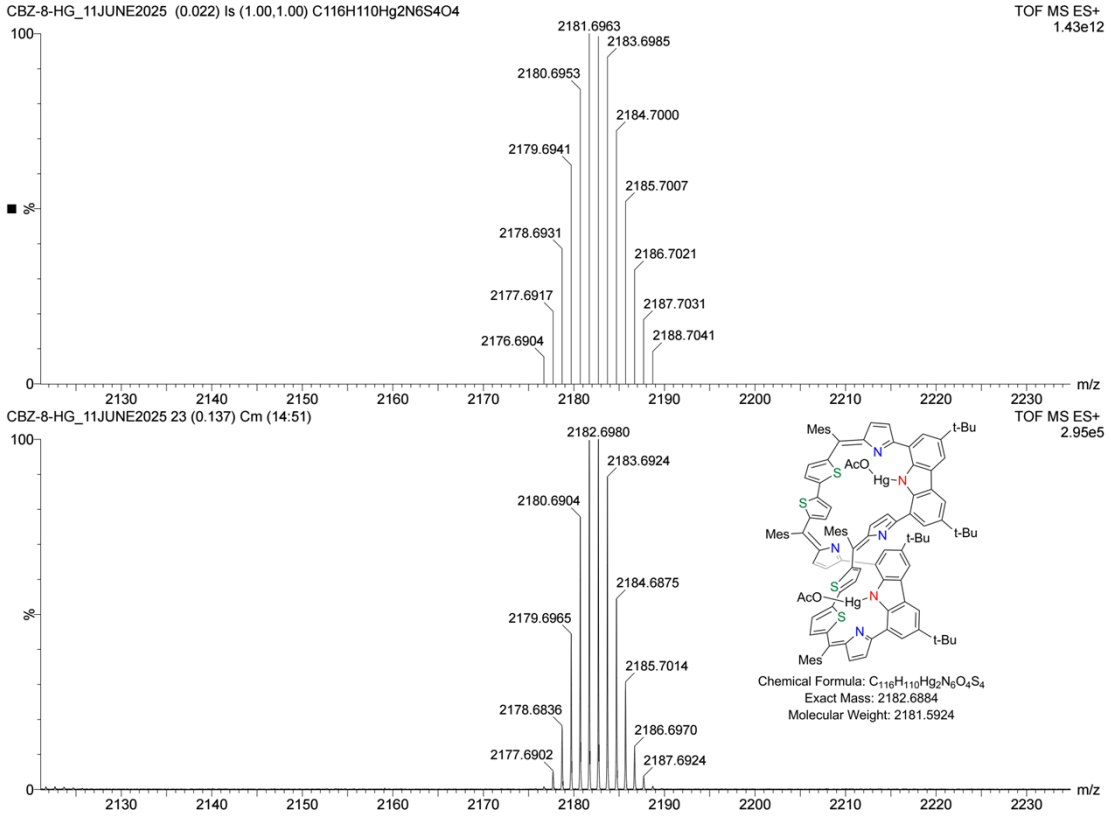

Figure S2. HR-MS (HESI) spectrum of **1-Ag. (**HESI = Heated Electrospray Ionization).

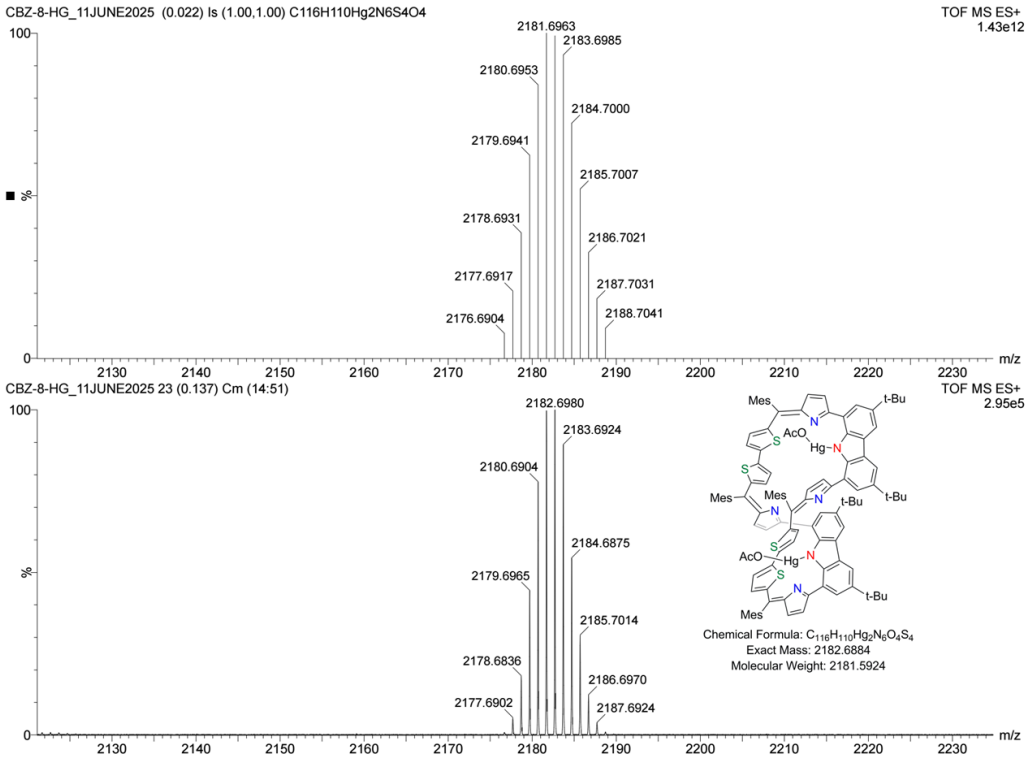

Figure S3. ESI-Mass spectrum of **1-Hg.**

4. NMR Spectra

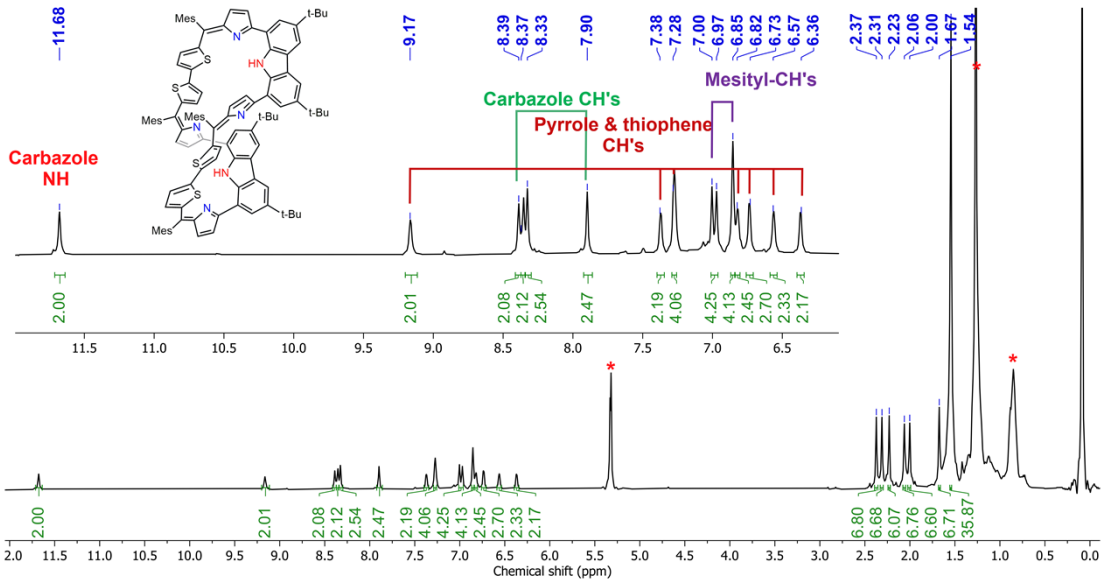

Figure S4. ^{1}H NMR of **1** recorded at 500 MHz in CD_2Cl_2 at 298 K. Signals marked with (*) denote residual solvents or impurities.

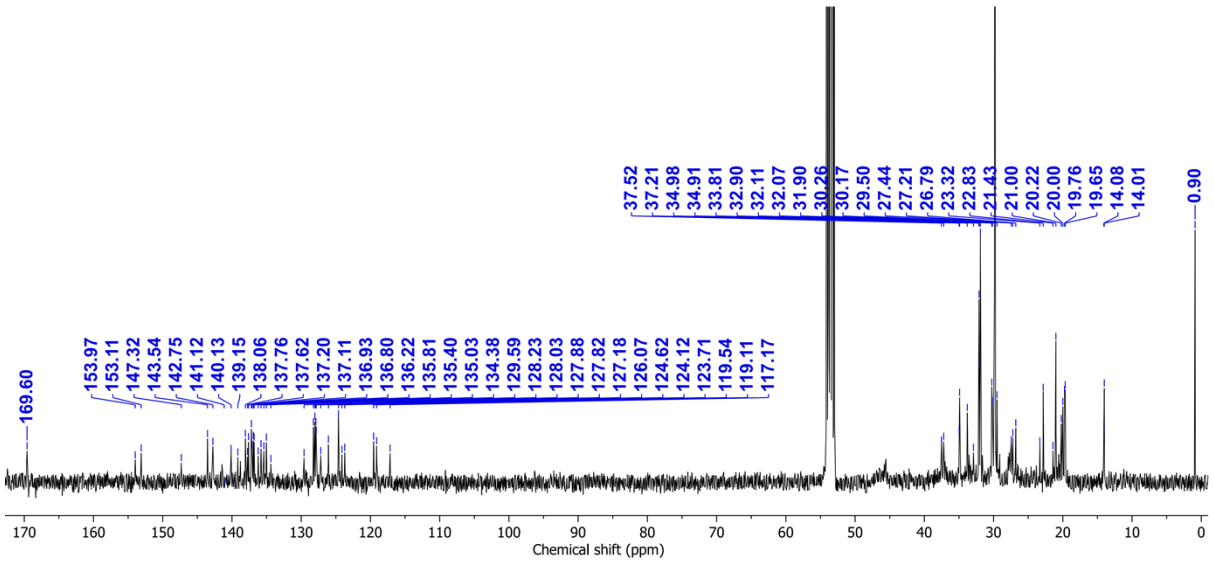

Figure S5. ^{13}C NMR of **1** recorded at 500 MHz in CD_2Cl_2 at 298 K.

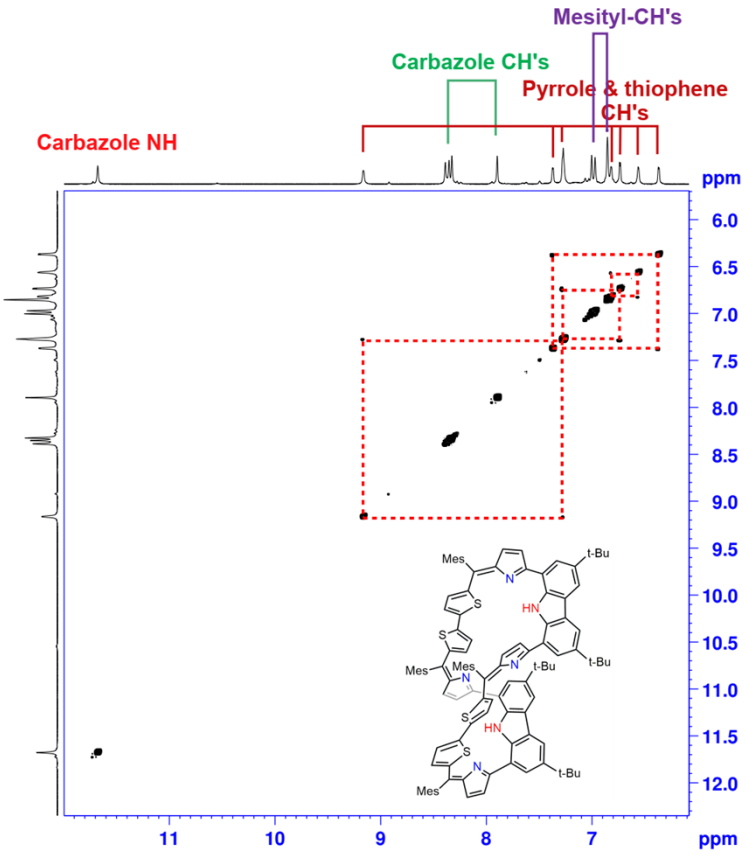

Figure S6. ^{1}H-^{1}H COSY spectrum of **1** recorded at 500 MHz in CD_2Cl_2 at 298 K.

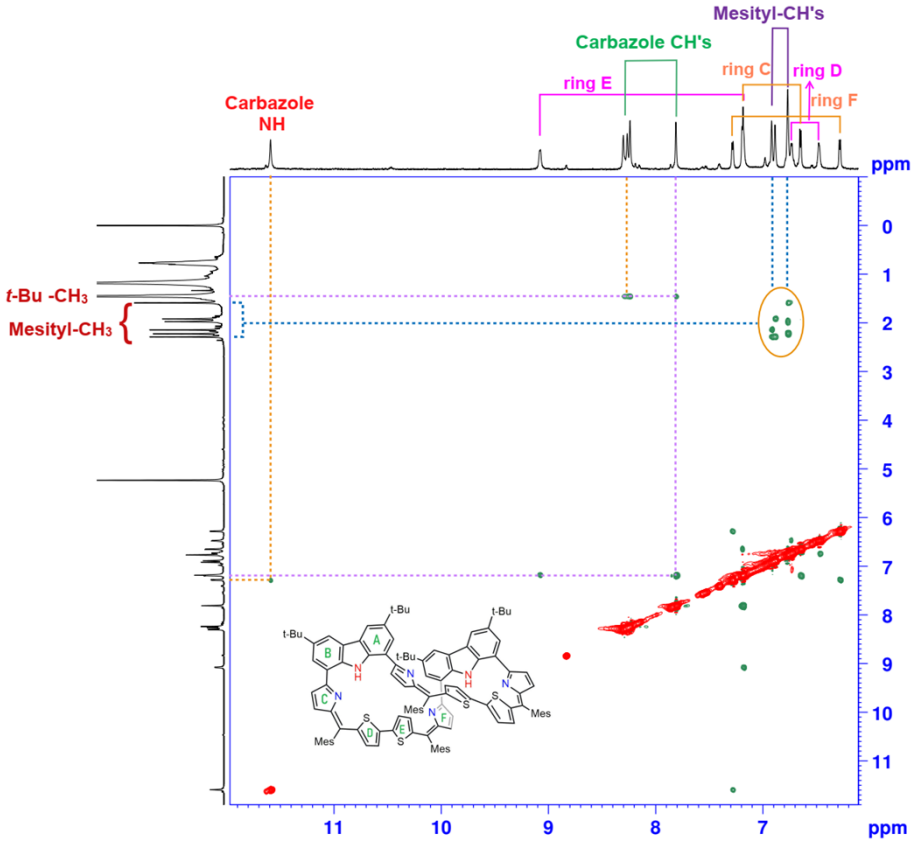

Figure S7. ^{1}H-^{1}H ROESY spectrum of **1** recorded at 500 MHz in CD_2Cl_2 at 298 K.

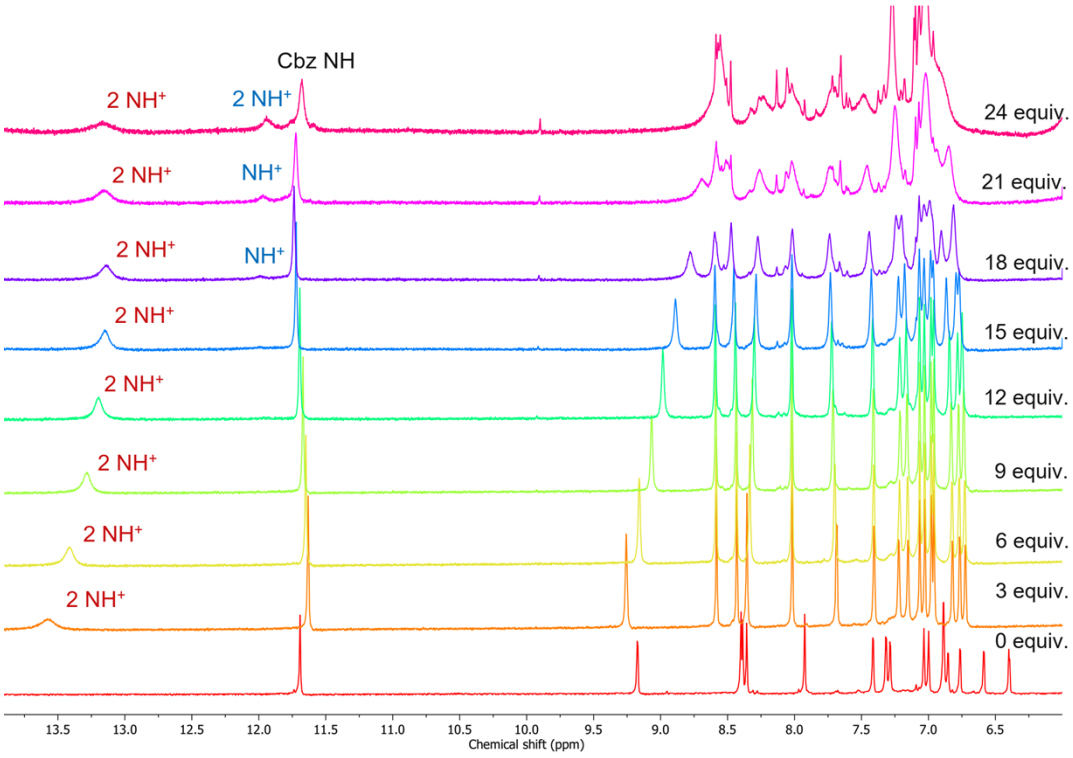

Figure S8. ^{1}H NMR spectra of **1** upon addition of increasing equivalence of CF_3COOH, recorded in CD_2Cl_2 at 273 K.

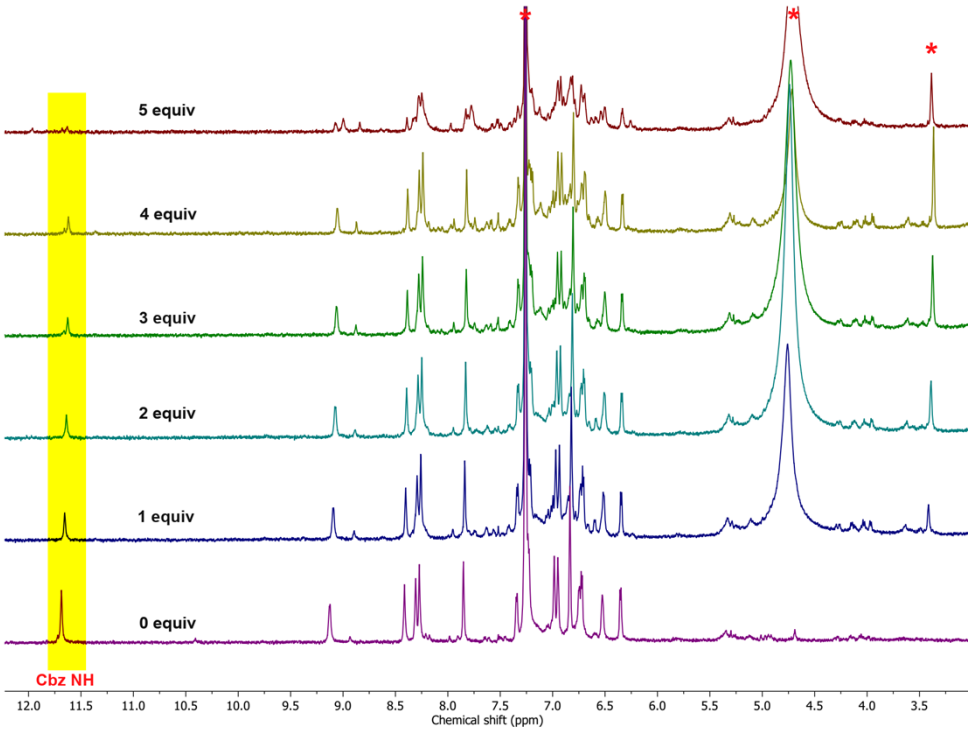

Figure S9. ^{1}H NMR spectra of **1** with various equivalents of Ag^+ in $CDCl_3$ at 298 K. Various equivalents of Ag+ were introduced by dissolving metal salt in MeOD. Signals marked with (*) denote residual solvents.

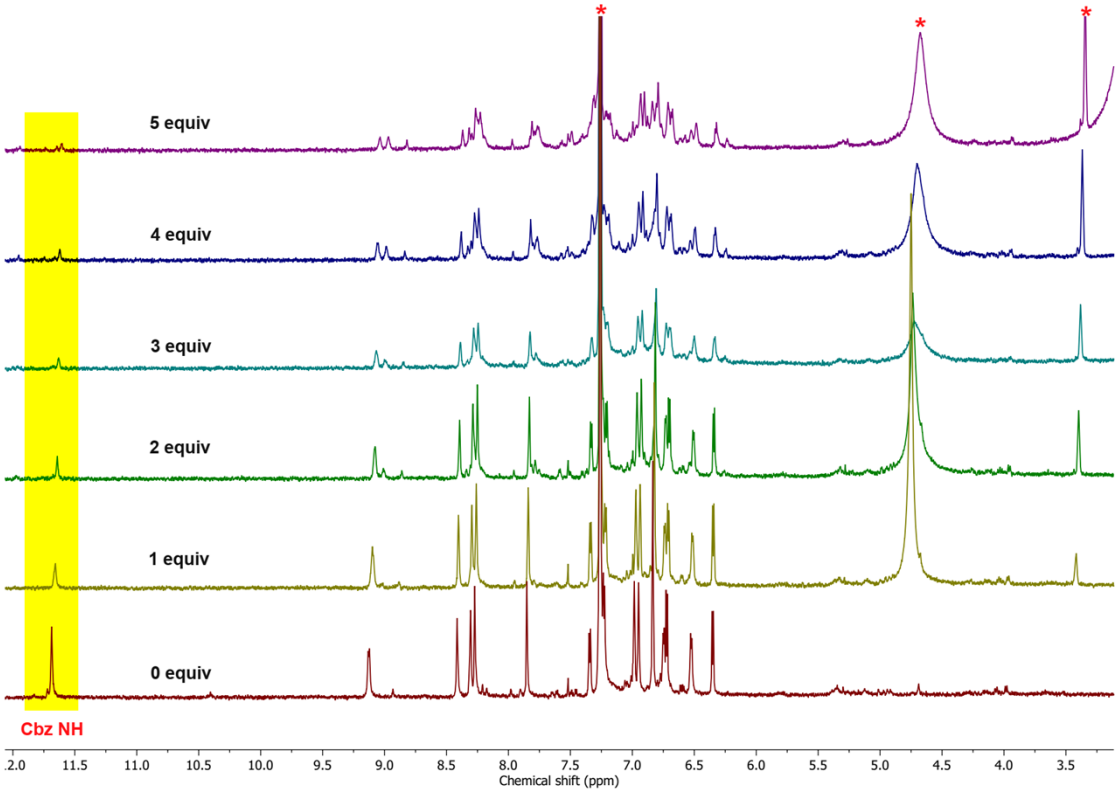

Figure S10. ^{1}H NMR spectra of **1** with various equivalents of Hg^{2+} in $CDCl_3$ at 298 K. Various equivalents of Hg^{2+} were introduced by dissolving metal salt in MeOD. Signals marked with (*) denote residual solvents.

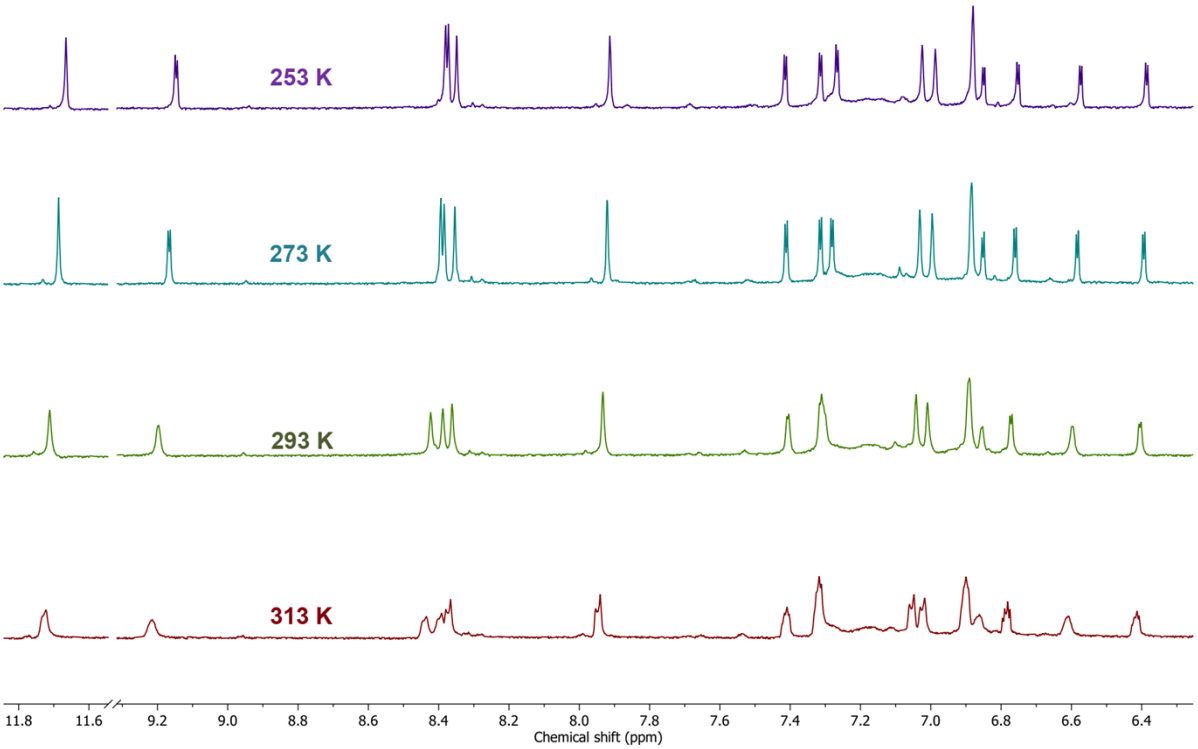

Figure S11. VT-NMR Spectra of **1** recorded at 500 MHz in CD_2Cl_2.

5. UV/Vis Absorption Spectra

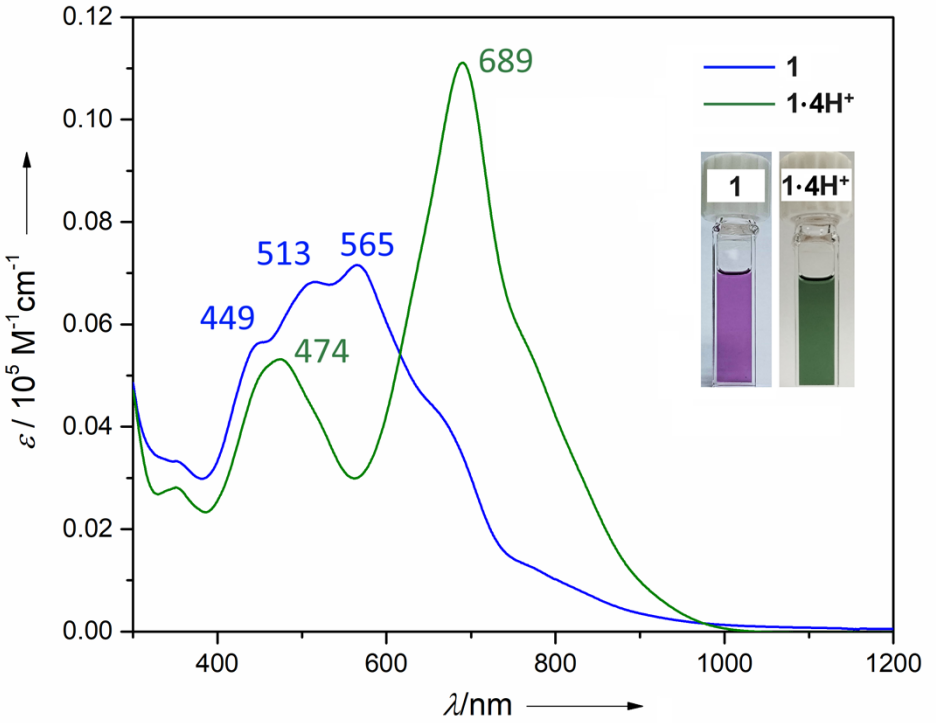

Figure S12. UV-Vis absorption spectra of **1** with its protonated form (diluted CF_3COOH used) recorded in CH_2Cl_2 at 298 K.

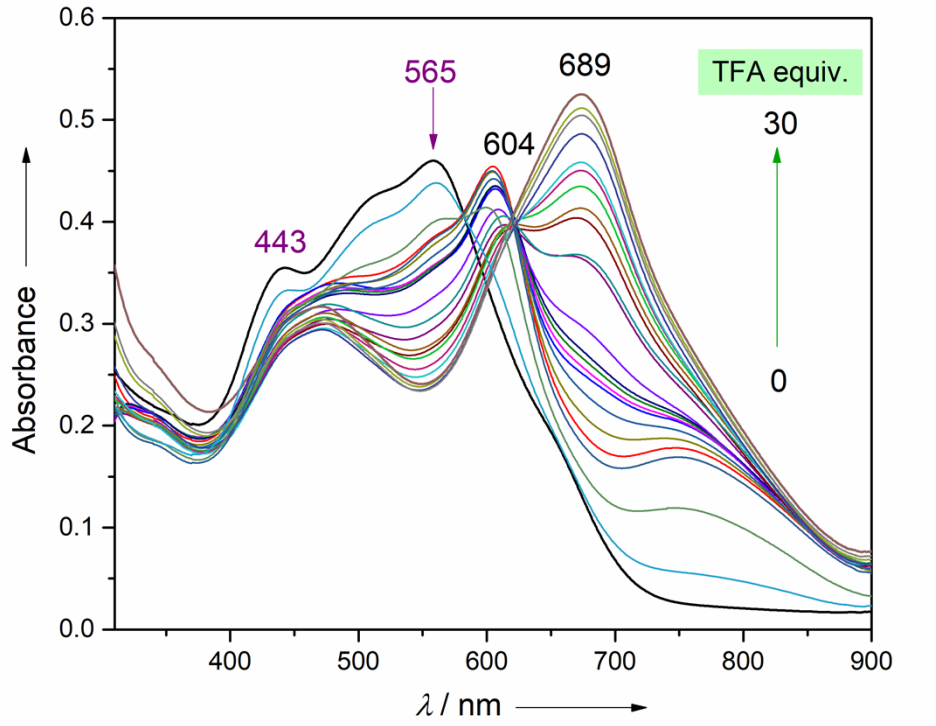

Figure S13. UV-Vis absorption spectra of **1** upon addition of increasing equivalence of CF_3COOH, recorded in CH_2Cl_2 at 298 K.

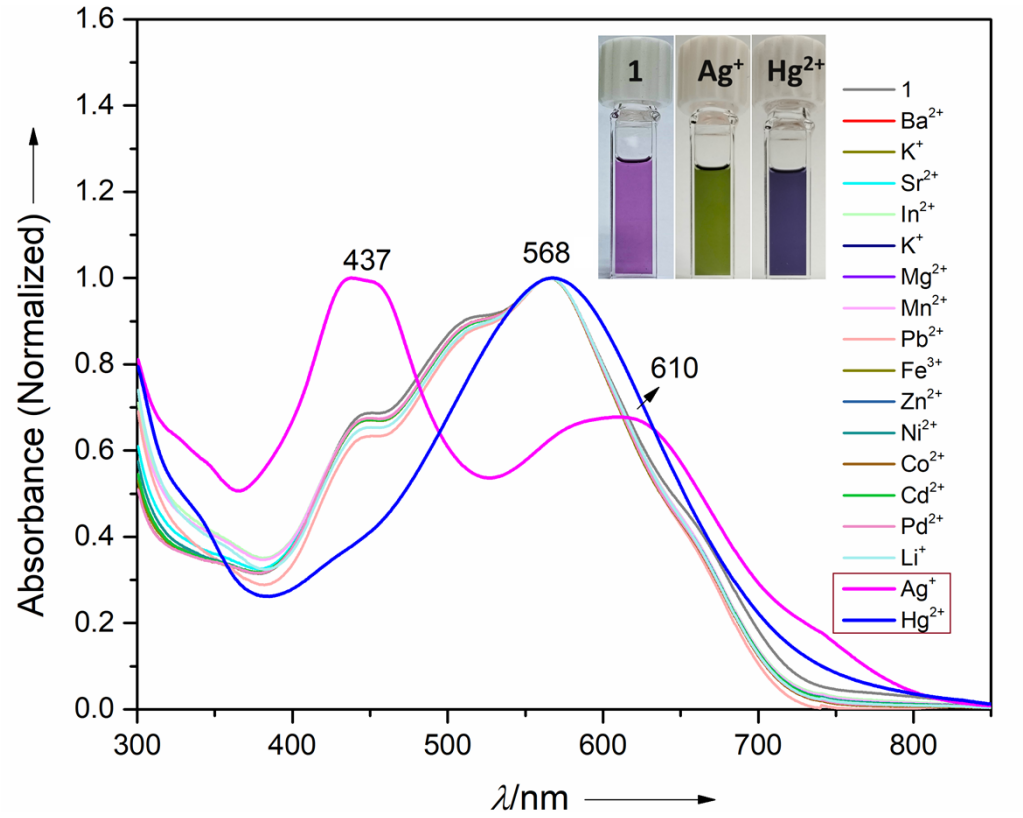

Figure S14. UV-Vis absorption changes of **1** (in CH_2Cl_2) upon addition of various metal ions (in CH_3OH).

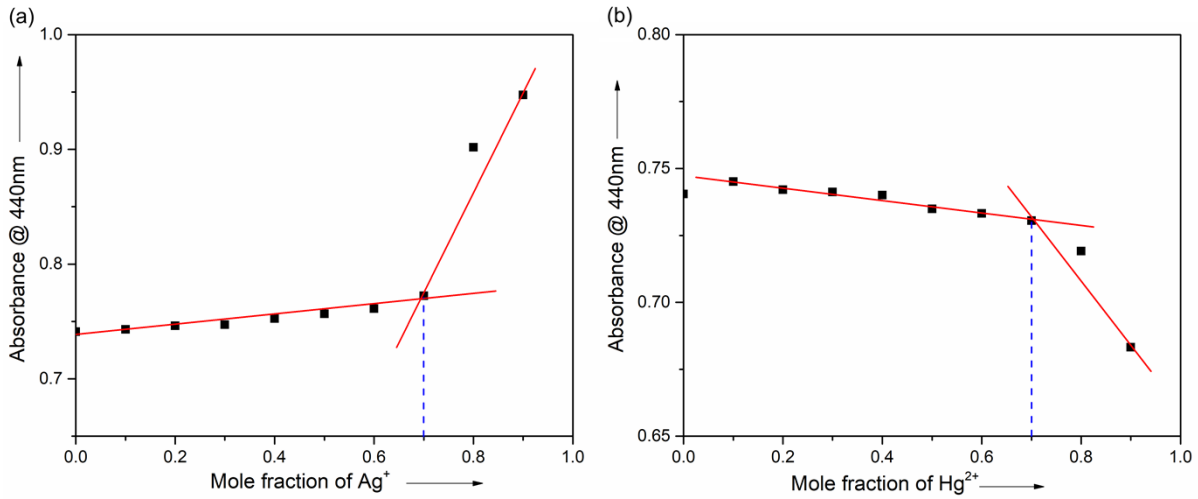

Figure S15. Job's plot for **1** (in CH_2Cl_2) with Ag^+ and Hg^{2+} ions (in CH_3OH).

6. Crystal Data

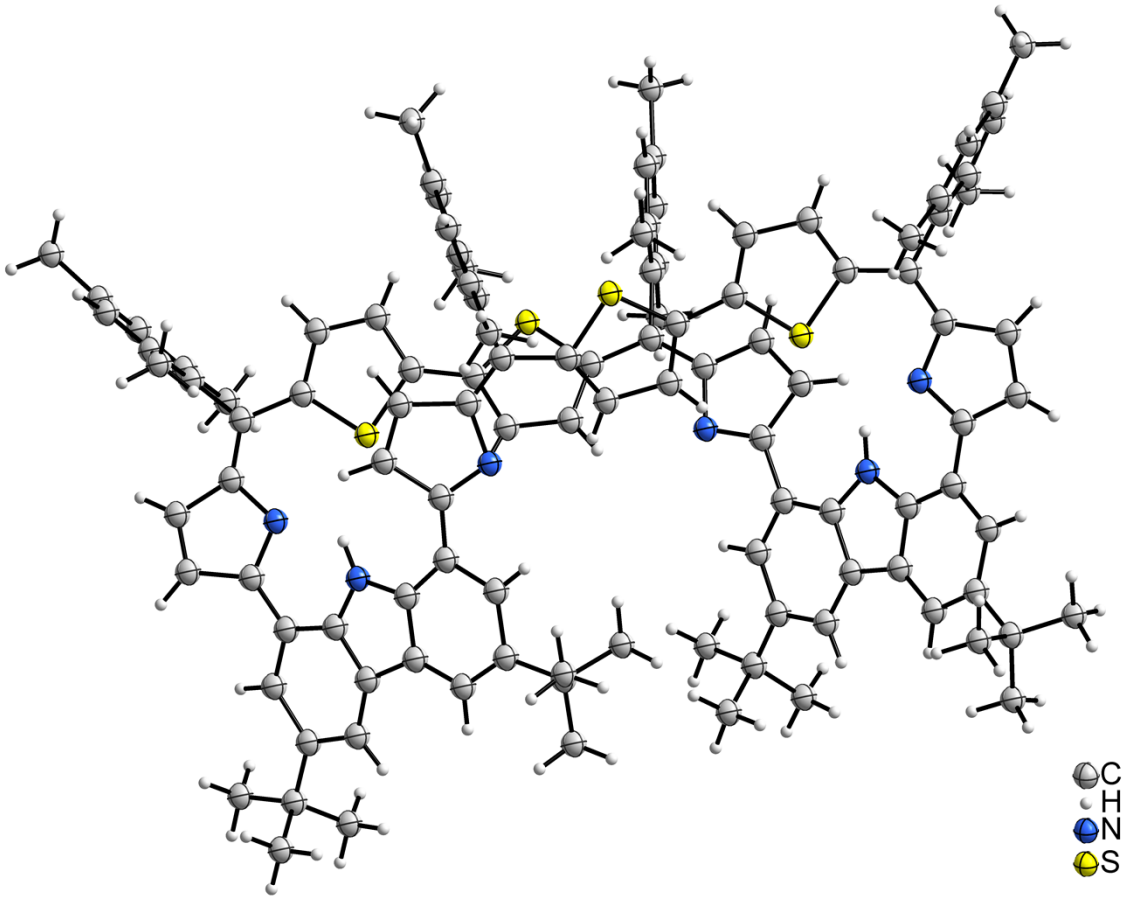

Figure S16. ORTEP drawing of **1**. The thermal ellipsoids are scaled to 50% probability level. Solvent molecules are omitted for clarity.

Method of Crystallization

Diffraction-grade crystals of **1** were grown by vapor diffusion of methanol into a THF solution of **1** at room temperature.

Table S1. Crystal data and structure refinements for **1.**

Compound	**1**
Empirical formula	$C_{112}\ H_{106}\ N_6\ S_4$
Formula weight	1664.26
Temperature/*K*	140(2) *K*
Crystal system	Monoclinic
Space group	P 21/n
a/Å	24.5514(16)
b/Å	15.9391(10)
c/Å	34.932(2)
α/°	90
β/°	101.616(2.
γ/°	90
Volume/Å^3	13389.8(15)
Z	4
ρ_{calc} Mg/m^3	0.826
μ/mm^{-1}	0.108
F(000)	3536
Crystal size/mm^3	0.460 x 0.143 x 0.086
Radiation	Mo*Kα* (λ = 0.71073)
2Θ range for data collection/°	2.043 to 26.373
Index ranges	-30<=h<=30, 0<=k<=19, 0<=l<=43
Reflections collected	17944
Independent reflections	7022 [R(int) = 0.1527]
Data/restraints/parameters	17944 / 110 / 1099
Goodness-of-fit on F^2	1.170
Final *R* indexes [*I*>=2σ (*I*)]	R1 = 0.1527, wR2 = 0.3981
Final *R* indexes [all data]	R1 = 0.2676, wR2 = 0.4310
Largest diff. peak/hole / e Å^{-3}	0.760 / -0.517
CCDC Number	2429004

7. DFT Calculations

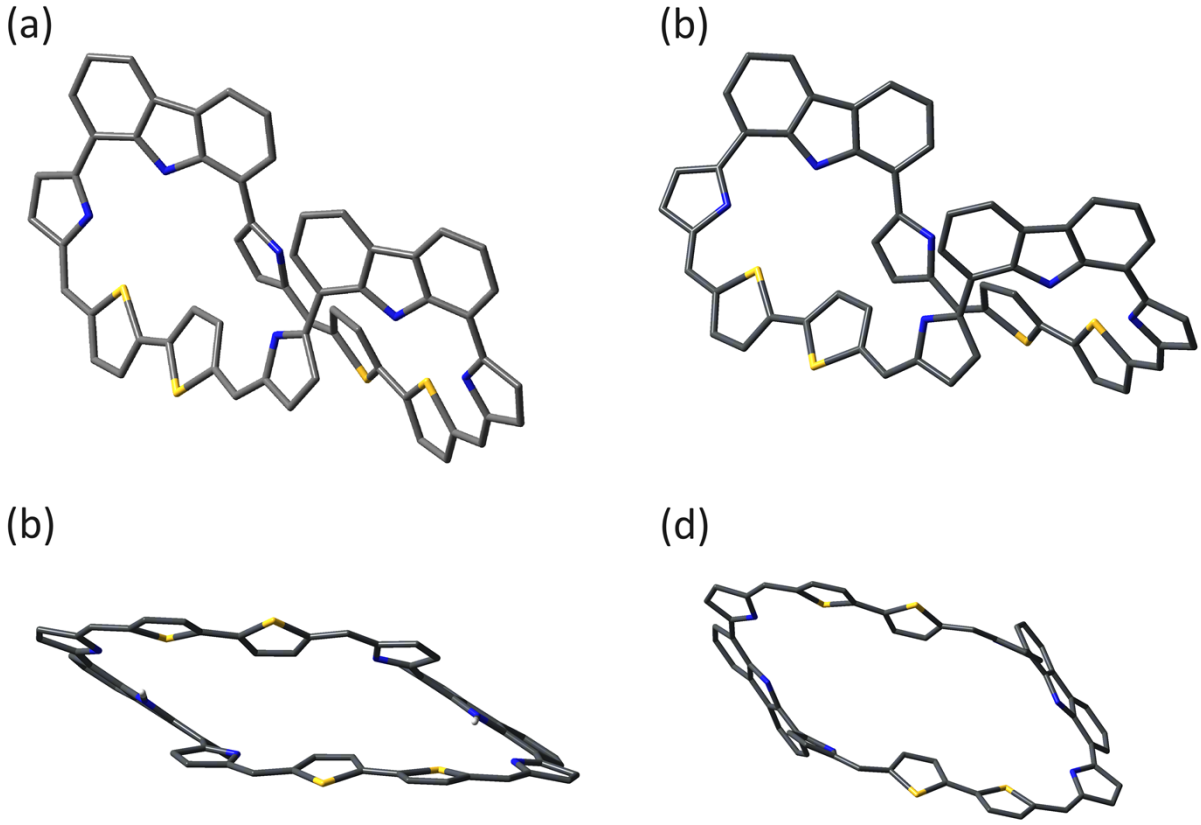

Figure S17. Optimized structures of (a) **1** and (b) **1⊃4H**$^{+}$ obtained by B3LYP/6-31G(d) method. Front views (top) and side views (bottom) are shown. For clarity, the *meso*-aryl groups, *tert*-butyl groups and hydrogens are omitted.

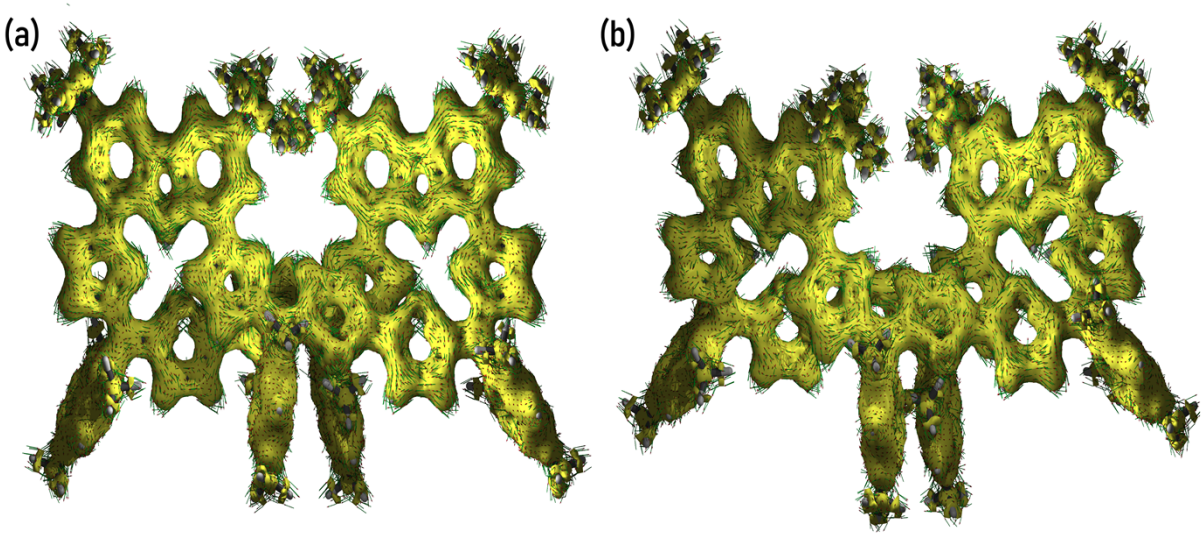

Figure S18. AICD plots of (a) **1** and (b) **1⊃4H**$^{+}$ at an isosurface value of 0.05 based on the optimized structures.

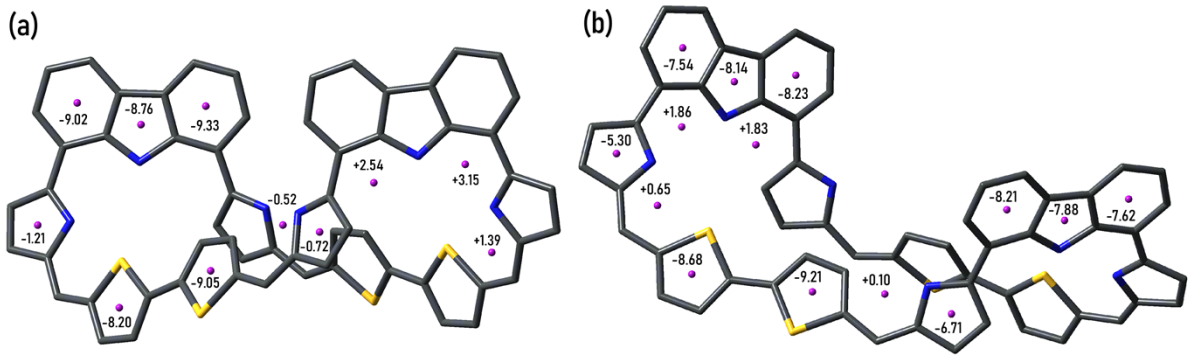

Figure S19. NICS (0) values computed at different points in the macrocycle (a) **1** (b) **1⊇4H**$^{+}$ based on the optimized structures at the B3LYP/6-31G(d) level. For clarity, the *meso*-aryl groups, tert-butyl groups and hydrogens are omitted, but they were all included for the calculations.

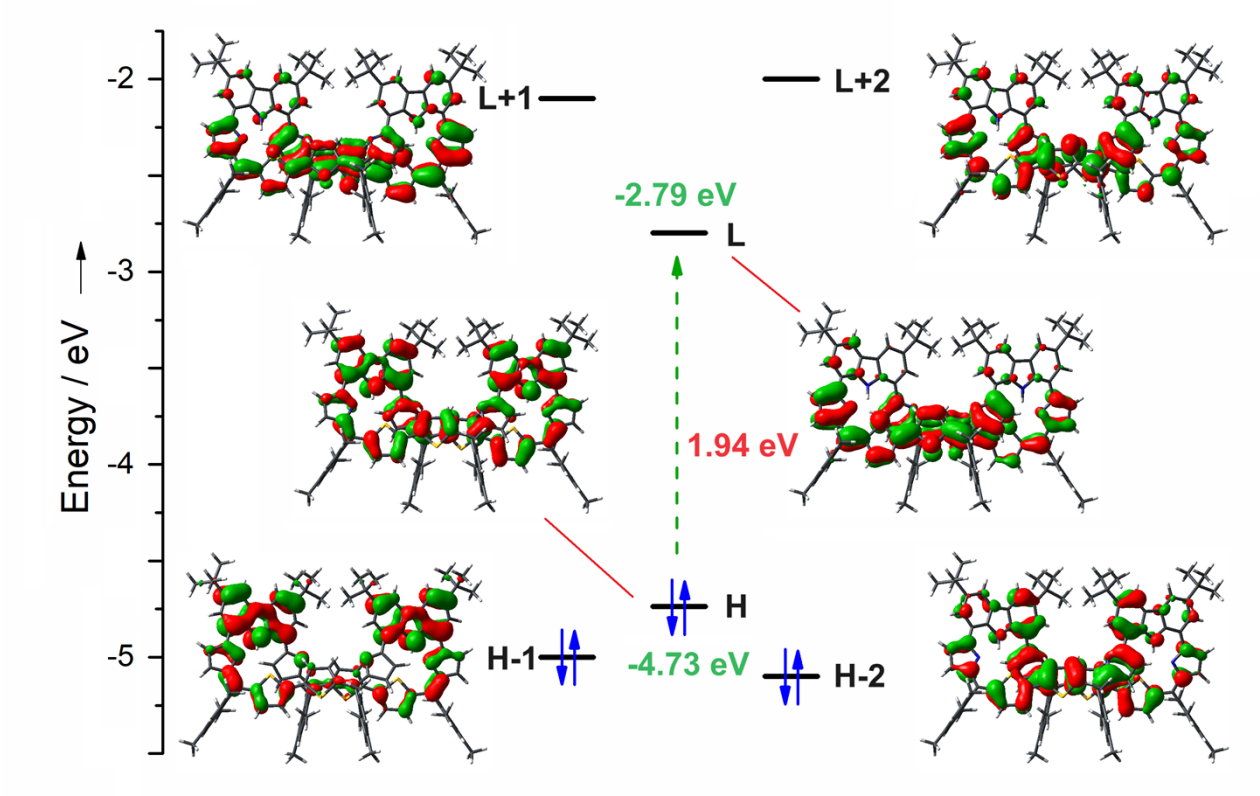

Figure S20. Energy level diagram of **1** with selected MOs.

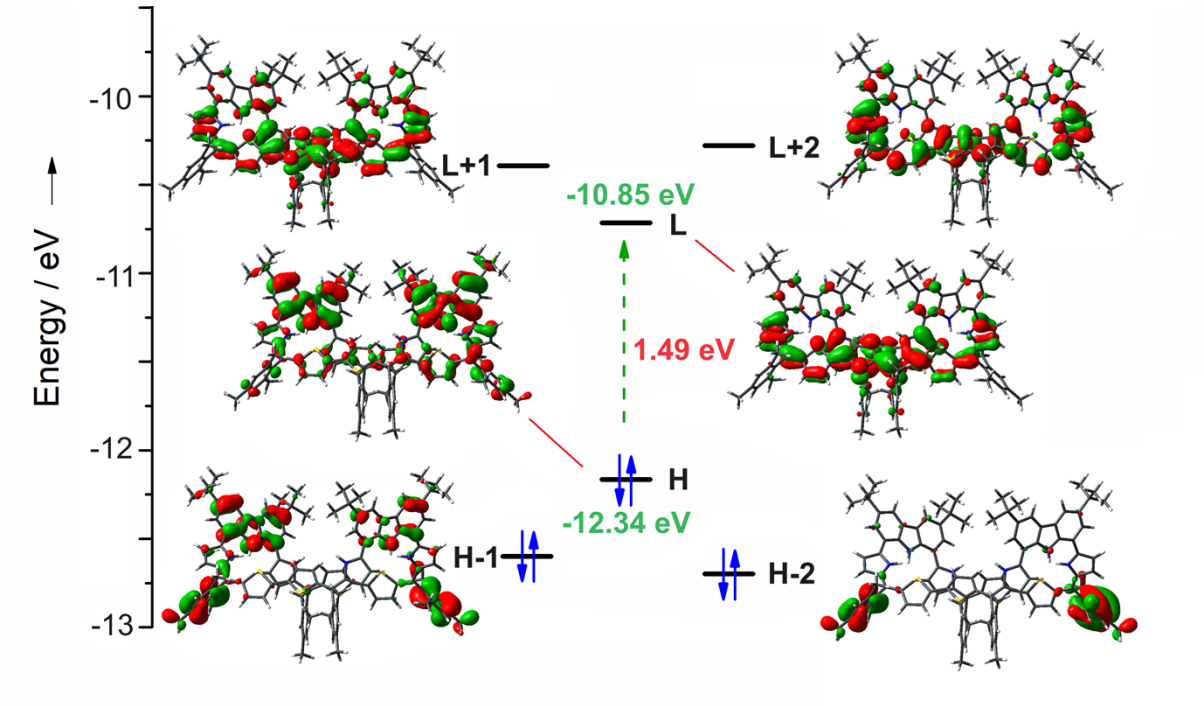

Figure S21. Energy level diagram of **1**·**4H**$^{+}$ with selected MOs.

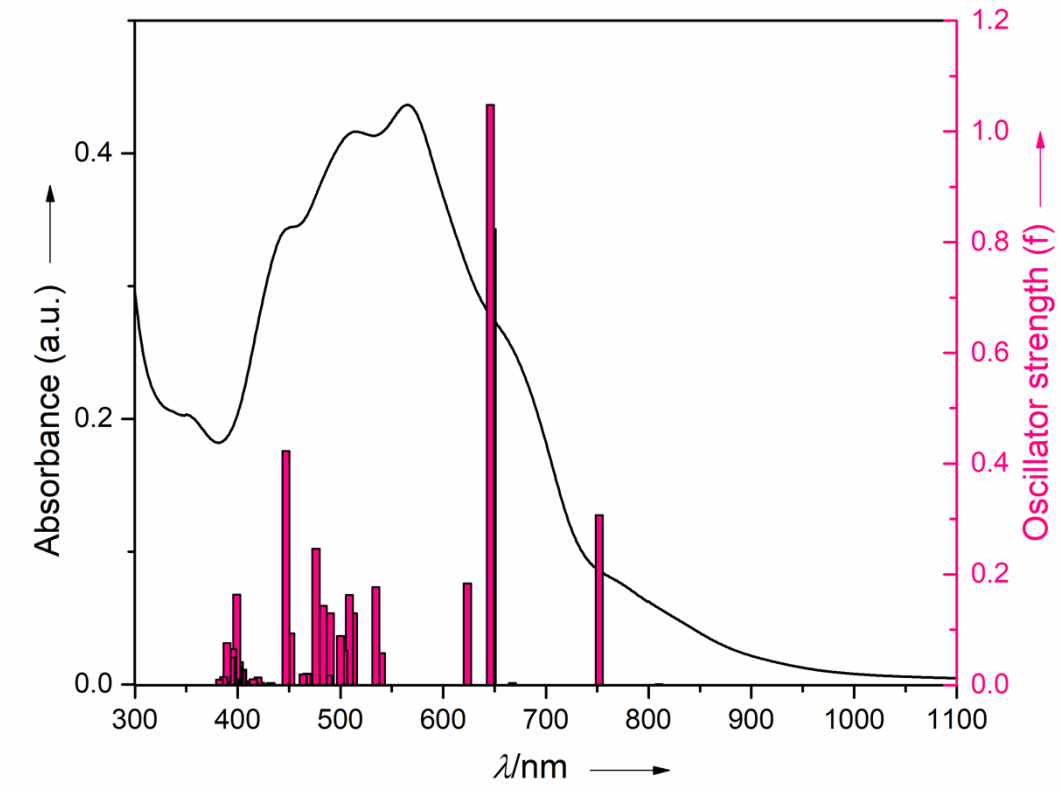

Figure S22. Calculated oscillator strength based on optimized structure (bar) and observed absorption spectra (line) of **1.**

Table S2: Selected transitions, oscillator strength, symmetry calculated for **1** from DFT analysis at B3LYP/6-31G(d) level of theory (H = HOMO, L= LUMO)

No.	Energy (cm^{-1})	Wavelength (nm)	Osc. Strength	Symmetry	Major contributions
1	12341.53	809.89	0.0018	Singlet-A	H→L (69.6%)
2	13300.88	751.82	0.3067	Singlet-A	H-1→L (20.9%), H→L+1 (66.3%)
3	14984.16	667.35	0.0038	Singlet-A	H-1→L+1 (69.3%)
4	15437.44	647.79	0.8238	Singlet-A	H-2→L (43.4%), H-1→L (53.3%)
5	15480.99	645.94	1.0478	Singlet-A	H-2→L (53.9%), H→L+1 (19.9%)
6	16035.90	623.59	0.1837	Singlet-A	H-2→L+1 (68.9%), H-1→L+3 (10.06%)
7	18527.36	539.74	0.0580	Singlet-A	H-4→L (10.1%), H-3→L (24.7%), H→L+2 (63.2%)
8	18709.64	534.48	0.1768	Singlet-A	H→L+3 (66.8%)
9	19502.48	512.76	0.1300	Singlet-A	H-5→L (17.03%), H-3→L (46.2%), H-3→L+1 (43.2%), H→L+3 (10.8%)
10	19658.15	508.69	0.1626	Singlet-A	H-3→L+1 (48.6%), H→L+2 (14.2%)
11	19871.88	503.23	0.0623	Singlet-A	H-4→L (65.3%),

					H-1→L+3 (17.1%)
12	20004.96	499.87	0.0888	Singlet-A	H-4→L+1 (58.8%),
13	20401.79	490.16	0.1300	Singlet-A	H-5→L (63.2%),
14	20481.64	488.25	0.0174	Singlet-A	H-5→L (11.2%), H-5→L+1 (63.8%), H-1→L+2 (13.6%)
15	20701.02	483.07	0.1430	Singlet-A	H-4→L+1 (32.5%), H-1→L+2 (56.1%)
16	21001.87	476.15	0.2467	Singlet-A	H-6→L (28.6%), H-5→L+1 (13.0%), H-1→L+3 (57.2%), H→L+2 (10.8%)
17	21389.82	467.51	0.0209	Singlet-A	H-5→L (12.9%), H-2→L+2 (67.3%)
18	21572.10	463.57	0.0196	Singlet-A	H-2→L+3 (68.2%)
19	22152.01	451.43	0.0936	Singlet-A	H-6→L+1 (64.4%)
20	22372.20	446.99	0.4230	Singlet-A	H-6→L (58.8%)
21	23126.33	432.41	0.0038	Singlet-A	H-12→L (35.3%), H-12→L+1 (15.9%), H-9→L (12.4%), H-9→L+1 (22.7%)
22	23164.24	431.70	0.0036	Singlet-A	H-12→L+1 (26.7%) H-11→L+1 (25.1%) H-9→L (45.1%) H-7→L+1(11.4%)

23	23179.56	431.42	0.0027	Singlet-A	H-12→L (10.7%) H-11→L (38.3%) H-11→L+1 (18.4%) H-9→L (14.3%) H-9→L+1 (34.5%) H-8→L (31.2%)
24	23214.24	430.77	0.0012	Singlet-A	H-11→L (29.5%) H-10→L (11.8%) H-8→L+1 (44.2%)
25	23683.66	422.24	0.0044	Singlet-A	H-10→L (53.8%)
26	23820.77	419.80	0.0137	Singlet-A	H-10→L+1 (50.0%)
27	24014.35	416.42	0.0031	Singlet-A	H-16→L (18.1%) H-16→L+1 (31.8%) H-15→L (16.0%) H-14→L (29.8%) H-13→L (24.1%) H-12→L (23.7%) H-10→L (18.3%) H-7→L (21.5%)
28	24085.32	415.19	0.0104	Singlet-A	H-16→L (45.0%) H-15→L+1 (15.2%) H-14→L+1 (23.9%) H-13→L+1 (21.2%) H-12→L+1(17.1 %) H-10→L+1 (16.5%) H-8→L+1 (10.7%)

					H-7→L+1 (20.0%)
29	24166.79	413.79	0.0006	Singlet-A	H-15→L (48.5%) H-15→L+1 (35.8%) H-15→L+2 (10.1%)
30	24204.69	413.15	0.0006	Singlet-A	H-14→L (25.1%) H-13→L+1 (41.2%)
31	24620.07	406.18	0.0073	Singlet-A	H-17→L (52.0%) H-14→L+1 (10.8%)
32	24649.91	405.68	0.0064	Singlet-A	H-19→L+1 (27.9%) H-18→L (43.3%) H-12→L (13.1%) H-11→L+1 (14.3%) H-7→L (13.3%)
33	24714.43	404.63	0.0279	Singlet-A	H-19→L (13.8%) H-18→L+1 (16.7%) H-17→L+1 (13.1%) H-16→L (19.9%) H-12→L+1 (10.8%) H-11→L (33.7%) H-11→L+1 (11.0%)
34	24758.80	403.90	0.0259	Singlet-A	H-17→L+1 (13.4%) H-16→L+1 (19.4%) H-15→L (10.7%) H-14→L (15.1%) H-13→L (10.7%)

					H-11→L+1 (32.9%) H-10→L+1 (14.3%) H-8→L+1 (17.7%) H-7→L+1 (13.2%)
35	24915.27	401.35	0.0413	Singlet-A	H-12→L (34.4%) H-11→L+1 (32.0%) H-7→L (20.2%) H-3→L+3 (14.2%)
36	24993.50	400.11	0.0337	Singlet-A	H-19→L (27.6%) H-18→L+1 (28.5%) H-17→L (11.0%) H-8→L+1 (17.1%) H-3→L+2 (35.9%)
37	25024.96	399.60	0.0335	Singlet-A	H-11→L (10.5%) H-3→L+2 (51.7%)
38	25066.09	398.95	0.1632	Singlet-A	H-17→L (21.2%) H-17→L+1 (15.4%) H-12→L+1 (31.7%) H-10→L (11.5%) H-10→L+1 (20.5%) H-7→L+1 (19.1%) H-4→L+2 (14.5%) H-3→L+2 (19.6%)
39	25171.75	397.27	0.0105	Singlet-A	H-19→L+1 (13.7%) H-18→L (19.8%)

					H-17→L+1 (45.7%) H-12→L+1 (10.7%) H-10→L (15.0%) H-3→L+3 (11.0%)
40	25308.06	395.13	0.0172	Singlet-A	H-17→L+1 (20.1%) H-16→L+1 (41.7%) H-3→L+3 (36.1%)
41	25327.42	394.83	0.0650	Singlet-A	H-15→L+1 (17.7%) H-14→L+1 (28.1%) H-13→L+2 (24.1%)
42	25417.75	393.43	0.0494	Singlet-A	H-16→L (12.5%) H-14→L (16.0%) H-13→L (11.9%) H-4→L+2 (11.1%) H-4→L+3 (15.7%) H-3→L+3 (41.4%)
43	25660.52	389.70	0.0760	Singlet-A	H-15→L+1 (11.6%) H-4→L+2 (58.9%)
44	25712.95	388.9	0.0046	Singlet-A	H-12→L (22.8%) H-12→L+1 (20.6%) H-8→L (33.4%) H-8→L+1 (28.7%)
45	25783.93	387.84	0.0006	Singlet-A	H-12→L+1 (29.8%) H-11→L+1 (17.2%) H-10→L (12.4%)

					H-9→L+1 (38.0%)
46	25878.29	386.43	0.0144	Singlet-A	H-17→L+1 16.7%) H-4→L+3 (59.3%)
47	26158.17	382.30	0.0096	Singlet-A	H-5→L+2 (64.1%) H-4→L+3 (20.5%)
48	26241.24	381.08	0.0008	Singlet-A	H-13→L (42.3%) H-13→L+1 (38.4%)
49	26310.61	380.08	0.0005	Singlet-A	H-15→L+1 (48.8%) H-14→L (19.4%)
50	26366.26	379.23	0.0015	Singlet-A	H-5→L+3 (65.7%)

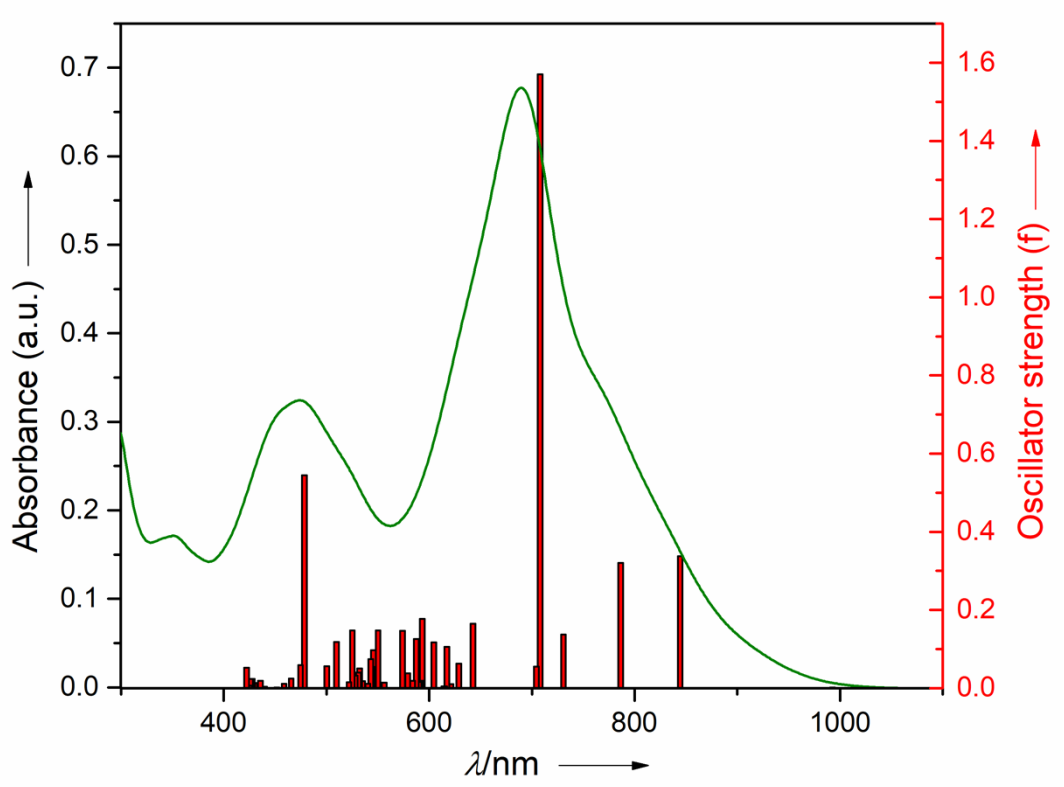

Figure S23. Calculated oscillator strength on the basis of optimized structure (bar) and observed absorption spectra (line) of **1⍰4H**$^{+}$.

Table S3: Selected transitions, oscillator strength, symmetry calculated for **1⍰4H**$^{+}$ from DFT analysis at B3LYP/6-31G(d) level of theory (H = HOMO, L= LUMO)

No.	Energy (cm^{-1})	Wavelength (nm)	Osc. Strength	Symmetry	Major contributions
1	10074.67	992.59	0.0013	Singlet-A	H→L (69.7%)
2	11844.25	844.31	0.3379	Singlet-A	H-2→L (16.5%), H→L+1 (66.6%)
3	127117.75	786.29	0.3200	Singlet-A	H-1→L (67.8%), H→L+1 (14.0%)
4	13686.42	730.66	0.1368	Singlet-A	H-3→L (10.9%), H-1→L+1 (67.4%)
5	14121.96	708.12	1.5700	Singlet-A	H-2→L (67.2%)
6	14200.19	704.23	0.0555	Singlet-A	H-2→L+1 (67.9%), H-1→L+1 (13.9%)
7	15561.66	642.61	0.1647	Singlet-A	H-5→L (11.9%), H-3→L (63.7%)
8	15900.41	628.91	0.0631	Singlet-A	H-5→L (14.7%), H-5→L+1 (15.8%), H-4→L (27.5%), H-3→L+1 (47.1%), H→L+2 (11.3%)
9	16093.98	621.35	0.0102	Singlet-A	H-5→L (43.4%),

					H-5→L+1 (12.4%), H-4→L+1 (17.5%), H→L+3 (10.3%)
10	16205.29	617.08	0.1057	Singlet-A	H-8→L (21.1%), H-7→L (18.6%), H-4→L+1 (18.3%), H-3→L+1(39.8%), H→L+2 (26.4%)
11	16261.75	614.93	0.0041	Singlet-A	H-8→L (41.2%), H-8→L+1 (28.6%)
12	16283.52	614.11	0.0048	Singlet-A	H-6→L (54.04%), H-6→L+2 (11.3%), H-6→L+3 (11.0%)
13	16538.39	604.66	0.1167	Singlet-A	H-11→L (10.7%), H-8→L (13.7%), H-5→L (16.4%), H-4→L (20.8%), H→L+2 (53.4%)

14	16852.95	593.37	0.1773	Singlet-A	H-11→L+1 (13.8%), H-9→L (12.6%), H-8→L (26.1%), H-7→L (26.2%), H-5→L (19.1%), H-4→L (34.1%), H-4→L+1 (14.0%)
15	16896.50	591.84	0.0191	Singlet-A	H-13→L (22.2%), H-13→L+1 (14.5%), H-10→L (38.6%), H-10→L+1 (10.1%), H-8→L (10.0%), H-4→L (11.2%)
16	16944.09	590.17	0.0156	Singlet-A	H-12→L+1 (14.4 %), H-11→L (38.9%), H-10→L (29.1%)
17	17024.75	587.38	0.1256	Singlet-A	H-13→L (28.9%), H-13→L+1 (15.1%), H-12→L+1 (22.5%), H-9→L (45.0%)

18	17126.37	583.89	0.0184	Singlet-A	H-12→L (12.2 %), H-8→L+1 (19.0%), H-7→L+1 (18.0%), H-5→L+1 (24.8%), H-4→L+1 (36.2%),
19	17267.52	579.11	0.0381	Singlet-A	H-13→L (25.2%), H-13→L+1 (15.5%), H-12→L (34.6%), H-11→L (19.3 %), H-9→L+1 (34.2%), H-3→L+1 (13.5%), H→L+3(13.3%)
20	17424.80	573.88	0.1465	Singlet-A	H-8→L+1 (11.9%), H-5→L+1 (16.21%), H-4→L+1 (21.2%), H-3→L (11.5%), H→L+3 (55.8%)
21	17978.09	556.24	0.0144	Singlet-A	H-12→L (18.5%), H-10→L (19.6%), H-9→L (30.7%), H-8→L+1 (17.8%), H-7→L+1 (20.7%), H-5→L (20.8%)
22	18173.28	550.26	0.1481	Singlet-A	H-8→L (21.3%) H-8→L+1 (10.3%) H-7→L (28.2%)

23	18323.30	545.76	0.0971	Singlet-A	H-13→L (17.1%) H-11→L (11.3%) H-8→L+1 (18.2%) H-7→L+1 (27.8%) H-6→L (15.5%) H-6→L+1 (22.9%) H-5→L (18.2%)
24	18365.24	544.50	0.0541	Singlet-A	H-9→L +1 (30.8%) H-7→L+1 (29.9%) H-5→L (15.9%)
25	18411.21	543.16	0.0738	Singlet-A	H-9→L+1 (35.4%) H-6→L (32.1%) H-6→L+1 (39.6%)
26	18506.39	540.35	0.0113	Singlet-A	H-9→L+1 (20.4%) H-8→L+1 (44.5%) H-7→L (19.9%)
27	18687.86	535.11	0.0175	Singlet-A	H-12→L (10.0%) H-12→L+1 (11.8%) H-11→L+1 (35.2%) H-10→L (31.3%) H-10→L+1 (18.3%) H-4→L+1 (12.0%) H-1→L+2 (35.8%)
28	18783.03	532.39	0.0508	Singlet-A	H-11→L (23.0%) H-11→L+1 (14.0%) H-10→L (13.3%)

					H-10→L+1 (44.3%) H-9→L+1 (10.2 %)
29	18826.59	531.15	0.0400	Singlet-A	H-11→L+1 (42.3%) H-10→L (12.4%)
30	18945.96	527.82	0.0323	Singlet-A	H-13→L+1 (14.9%) H-12→L (26.7%) H-12→L+1 (51.8%)
31	19041.13	525.17	0.1477	Singlet-A	H-13→L+1 (58.3%)
32	19160.50	521.9	0.0146	Singlet-A	H-1→L+3 (68.2%)
33	19613.78	509.85	0.1184	Singlet-A	H-12→L+1 (10.3%) H-2→L+2 (60.5%)
34	19992.87	500.17	0.0561	Singlet-A	H-14→L+1 (15.0%) H-2→L+3 (66.3%)
35	20900.24	478.47	0.5451	Singlet-A	H-14→L (60.2%) H-2→L+2 (28.2%) H→L+3 (12.1%)
36	21065.58	474.70	0.0586	Singlet-A	H-14→L+1 (63.4%) H-3→L+2 (14.8%)
37	21475.31	465.65	0.0249	Singlet-A	H-5→L+2 (11.5%) H-3→L+2 (63.2%)
38	21798.74	458.75	0.0115	Singlet-A	H-7→L+2 (17.5%) H-5→L+3 (11.2%) H-3→L+3 (54.4%)
39	22145.56	451.55	0.0013	Singlet-A	H-8→L+3 (18.8%) H-7→L+3 (23.8%)

					H-5→L+2 (43.4%)
40	22217.34	450.10	0.0005	Singlet-A	H-8→L+2 (37.2%) H-7→L+3 (13.5%) H-5→L+3 (20.6%)
41	22230.25	449.84	0.0010	Singlet-A	H-8→L+3 (25.4%) H-7→L+2 (37.8%)
42	22258.48	449.27	0.0001	Singlet-A	H-7→L+2 (29.5%) H-6→L+2 (33.2%) H-6→L+3 (29.2%) H-5→L+3 (17.7%)
43	22746.44	439.63	0.0037	Singlet-A	H-8→L+2 (29.7%) H-7→L+2 (21.1%) H-5→L+2 (31.4%) H-4→L+2 (42.8%) H-3→L+3 (15.0%)
44	22958.57	435.57	0.0193	Singlet-A	H-15→L (35.3%) H-8→L+3 (22.7%) H-7→L+3 (18.5%) H-5→L+3 (22.2%) H-4→L+3 (32.7%)
45	23248.93	430.13	0.0129	Singlet-A	H-15→L (12.7%) H-9→L+2 (47.2%) H-5→L+3 (12.6%) H-4→L+3 (20.9 %)
46	23353.78	428.20	0.0115	Singlet-A	H-15→L (16.9%)

					H-11→L+2 (50.1%) H-10→L+3 (25.2%)
47	23384.43	427.63	0.0236	Singlet-A	H-11→L+2 (15.7%) H-11→L+3 (16.3%) H-10→L+2 (41.2%) H-10→L+3 (17.4%) H-9→L+2 (20.3%) H-5→L+3 (10.2%) H-4→L+3 (21.0%)
48	23486.05	425.79	0.0236	Singlet-A	H-15→L (36.8%) H-13→L+2 (43.5%) H-11→L+3 (10.2%) H-10→L+2 (13.2%)
49	23510.25	425.35	0.0069	Singlet-A	H-10→L+2 (45.4%) H-10→L+3 (25.8%) H-4→L+. (11.1%)
50	23680.43	422.29	0.0526	Singlet-A	H-16→L (66.0%) H-15→L (12.2%)

8. Cartesian coordinates of optimized geometries and minimized energies

Table S4: Cartesian coordinates of the S0 optimized geometry of the macrocycle **1** optimized at B3LYP/6-31G(d) level of theory

Sum of imaginary frequencies = 0

Total Energy (hartree) = -6253.131621 Hartrees

Optimized structure Coordinates:

Chemical Symbol	Coordinates (Angstroms)		
	X	Y	Z

S	0.000000235	-0.000001684	-0.000003115
S	0.000000772	-0.000001773	0.000000138
S	-0.000000951	-0.000002615	0.000001669
S	0.000001352	-0.000000842	-0.000004792
N	0.000001151	-0.000000588	-0.000002989
N	0.000000585	0.000000446	-0.000000253
C	0.000002969	0.000001525	-0.000001787
N	-0.000000066	-0.00000074	0.000000473
N	-0.000001598	0.000000299	0.000003184
N	-0.000003593	-0.000000964	0.000006579
C	-0.000001453	-0.00000063	-0.000000973
C	-0.000000291	0.000001011	0.000000639
C	0.000001745	-0.00000063	-0.000000461
C	-0.000000975	0.000002562	-0.000004409
C	-0.000002583	0.000000358	0.000003408
C	0.00000129	0.000001043	0.000000289
C	0.000000174	0.000000437	-0.000000828
C	0.000000804	-0.000000055	-0.000000723
C	-0.000001493	-0.000002261	-0.00000498
C	0.00000202	0.000001561	-0.000001562
C	0.000001196	0.000002842	0.000003685
C	-0.000004014	0.000000722	-0.000000073
C	0.000000552	-0.000001809	0.000000277
C	0.00000385	0.000000317	0.000001699
C	0.000001504	0.000001477	0.000001158
C	0.000009292	0.000003468	-0.000005968
C	0.000000752	-0.000000653	-0.000000893
C	0.000001122	-0.000001244	0.00000159
C	-0.000000382	-0.000000951	-0.000000522
C	0.000001011	-0.000004761	-0.000000954
C	0.000001136	0.000000604	0.000000343
C	-0.000000229	-0.000000626	0.000000616
C	0.00000167	-0.000002627	0.000003001
C	0.0000006	-0.000000064	0.000000167
C	-0.000000304	0.000004726	-0.000000548
C	-0.00000878	0.000003215	0.0000059
C	-0.000001695	0.000002508	-0.000002955
C	0.000000401	-0.000001508	0.000002114
C	-0.000003167	-0.000001906	0.000000748
C	0.000000069	-0.000000094	0.000000017
C	0.000000438	0.000000338	-0.00000108
C	-0.000000506	0.000000689	0.000002103
C	-0.000002694	0.000001034	0.000000762
C	0.000001061	0.000003938	-0.000000665
N	0.000003451	-0.000001138	-0.000005809
C	-0.00000059	-0.00000071	0.000000175
C	0.000000132	0.000000963	-0.000000435
C	0.000000537	-0.000002134	-0.00000025

C	-0.000000504	0.000000013	0.000001347
C	-0.000001122	0.000002012	-0.000001791
C	0.000001233	0.000000055	0.000000372
C	-0.000000608	0.000003719	0.000005202
C	0.000000321	-0.000001109	-0.000000146
C	-0.000001079	-0.000000091	0.000001073
C	-0.000000351	-0.000001192	-0.000001524
C	-0.000001763	0.000002304	0.000003807
C	0.000000515	0.000000747	-0.000001452
C	0.000000182	0.000000535	0.000000944
C	-0.000001952	0.000000946	-0.000000529
C	-0.000000734	-0.000000031	-0.000000239
C	-0.000000343	0.000000477	-0.000000557
C	0.00000159	-0.00000314	0.000000753
C	-0.000001079	0.000001271	-0.000000387
C	-0.000000363	0.000000911	-0.000000246
C	-0.0000001	-0.000001303	0.00000027
C	0.000000087	-0.000001505	-0.000000531
C	-0.000000695	-0.000001383	-0.000003106
C	-0.0000001	-0.000001552	0.000000478
C	-0.000000858	-0.000000678	-0.000000227
C	0.000000787	-0.000000101	-0.000001234
C	0.000000329	-0.000000062	0.000000283
C	-0.000000202	0.000000473	0.000000818
C	-0.000000069	0.000000197	0.000000374
C	-0.000000702	-0.000002066	-0.000000039
C	0.000000092	0.000000728	-0.000000351
C	0.000001244	-0.00000059	0.000000054
C	-0.000001286	0.000000109	-0.000000677
C	-0.00000006	0	0.000000197
C	0.000000316	0.000000037	0.000000123
C	-0.000001132	0.000004024	0.00000049
C	-0.000000003	-0.000000021	0.000000027
C	-0.000001736	-0.000003249	-0.000000739
C	0.000002705	0.000000966	-0.000000694
C	-0.000000277	0.000000081	-0.00000019
C	0.000001218	0.000001942	0.000001624
C	-0.000001223	-0.000000638	-0.000000147
C	0.000000071	-0.00000003	0.000000211
C	0.000000655	-0.000001129	-0.000000288
C	0.000000932	-0.000000468	-0.000000651
C	-0.00000143	0.000000098	0.000000238
C	-0.000000966	-0.000000762	-0.000003785
C	0.000001347	0.000000069	-0.000002416
C	0.000000966	0.000000882	0.000000598
C	-0.000001892	-0.000000481	0.000000102
C	0.000003519	-0.000002049	-0.000001728
C	0.000001607	0.000002681	0.000003779

C	-0.000000322	0.000000003	-0.000000049
C	-0.000000812	0.000000689	-0.000000461
C	0.000001356	-0.000000039	0.000000613
C	0.000000349	-0.000000442	0.00000064
C	-0.000002933	0.000001477	0.000001784
C	-0.000001295	-0.00000481	0.00000124
C	-0.000000639	0.000000347	0.000000986
C	0.00000036	-0.000000022	-0.000000379
C	0.000001147	0.000000645	0.000000629
C	-0.000000936	-0.00000012	0.000001196
C	0.00000002	-0.000000187	0.00000061
C	-0.000000101	0.000000072	0.000000434
C	-0.000000716	-0.000000158	-0.000000529
C	0.00000024	0.000000794	-0.000000066
C	-0.000000446	-0.000000323	-0.000001531
C	0.000000584	0.000001916	0.000001804
C	0.000000396	-0.000000347	-0.000000237
C	-0.000000149	-0.000000152	0.000000301
C	0.000000406	-0.00000032	0.000001595
C	-0.000000441	-0.000000375	0.000000298
C	-0.000000634	0.000001895	-0.000001703
C	0.000000107	-0.000000164	-0.0000002
C	-0.000000065	-0.00000021	-0.000000276
C	0.000000086	0.000000584	0.000000948
C	0.000000466	-0.000000053	-0.000000248
C	-0.000000277	0.000000552	-0.000000537
H	-0.000000837	0.000000124	0.000002858
H	-0.000000052	-0.000001073	-0.000001047
H	0.000001422	0.000000421	-0.000002488
H	-0.000000528	-0.000000172	-0.000000292
H	0.000000417	0.000000217	-0.000000108
H	-0.000000054	-0.000000061	0.000000077
H	-0.000000277	0.000000023	0.000000019
H	-0.00000023	-0.00000005	-0.00000021
H	0.000000111	-0.000000358	-0.00000006
H	-0.000000428	-0.000000541	0.000000125
H	0.000000022	0.000000153	0.000000237
H	-0.000000252	-0.000000027	0.000000506
H	-0.00000004	-0.00000038	-0.000000052
H	-0.000000093	-0.000000222	0.000000221
H	-0.000000634	0.000000116	0.000000293
H	0.000000121	0.000000238	-0.000000213
H	0.000000039	0.000000041	-0.000000119
H	0.000000361	0.000000216	-0.000000003
H	0.000000349	0.000000107	0.000000187
H	0.000000125	-0.000000006	-0.000000048
H	0.000000386	-0.000000425	-0.000000367
H	-0.000000108	0.000000086	-0.000000023

H	-0.000000117	0.000000229	0.000000107
H	-0.000000109	0.000000204	0.000000099
H	0.000000049	-0.000000091	-0.000000099
H	0	0.000000287	-0.000000323
H	-0.000000102	-0.000000004	-0.000000031
H	0.000000031	0.000000079	0.000000003
H	-0.000000108	-0.000000581	-0.000000298
H	0.000000062	0.000000536	0.000000127
H	-0.00000023	0.000000051	-0.000000017
H	0.000000434	0.000000018	0.000000394
H	0.000000612	-0.000000202	-0.000000014
H	-0.000000243	-0.000000063	-0.000000172
H	-0.000000077	0.000000419	-0.000000305
H	0.000000324	0.000000057	0.000000089
H	-0.000000037	-0.000000069	-0.000000153
H	0.000000076	-0.000000013	0.000000039
H	-0.000000082	0.00000005	-0.000000236
H	0.000000065	-0.000000238	-0.000000139
H	-0.000000045	-0.000000147	0.00000018
H	0.000000248	-0.000000106	-0.000000276
H	0.00000031	-0.000000344	0.000000165
H	-0.000000007	-0.000000369	0.000000137
H	0.00000006	-0.000000102	0.000000099
H	-0.000000067	-0.000000057	-0.000000118
H	0.000000007	0.000000042	0.000000219
H	0.000000011	0.000000485	-0.000000227
H	0.000000025	0.000000025	-0.00000009
H	0.000000179	-0.000000639	0.000000197
H	-0.000000029	0.000000248	-0.000000108
H	-0.000000034	-0.000000234	-0.000000245
H	0.00000006	0.000000107	-0.000000459
H	0.000000109	0.000000262	-0.000000247
H	-0.0000001	0.000000021	-0.000000254
H	0.000000486	-0.000000114	0.000000267
H	0.000000522	0.00000004	0.000000131
H	-0.000000323	0.000000303	-0.000000015
H	-0.000000129	-0.000000317	0.000000156
H	0.000000194	0.000000003	0.000000105
H	0.00000036	0.000000339	0.000000349
H	-0.000000145	0.000000326	-0.000000016
H	0.000000259	-0.00000002	-0.000000012
H	-0.000000439	-0.00000003	-0.00000044
H	-0.000000734	-0.000000257	-0.000000049
H	0.000000652	0.000000098	-0.000000294
H	-0.000000102	-0.000001211	0.000001081
H	0.00000026	-0.000000097	-0.000000269
H	-0.000000544	-0.000000162	-0.000000209
H	-0.000000073	-0.00000003	0.000000173

H	0.000000015	-0.000000063	-0.000000116
H	-0.00000009	0.00000009	0.000000089
H	0.000000026	-0.000000057	-0.000000003
H	0.000000192	-0.000000184	0.000000198
H	0.00000004	-0.000000001	0.000000172
H	0.000000084	-0.000000032	0.000000145
H	-0.000000075	-0.000000231	0.000000092
H	0.000000177	-0.000000378	0.000000116
H	-0.000000251	-0.000000011	0.000000104
H	-0.000000144	-0.000000212	-0.000000241
H	0.000000353	-0.00000026	-0.000000259
H	0.000000178	-0.000000466	0.000000171
H	-0.0000002	0.000000124	0.000000245
H	-0.000000459	-0.000000259	0.000000086
H	-0.000000049	0.000000344	-0.000000116
H	-0.000000248	-0.000000112	0.00000016
H	-0.000000015	0.000000003	0.000000127
H	-0.000000019	-0.000000016	-0.000000035
H	0.000000167	0.000000075	-0.000000173
H	0.000000434	-0.000000295	-0.000000045
H	0.000000004	0.000000305	0.000000191
H	0.000000103	-0.000000232	0.000000339
H	-0.000000429	-0.000000241	0.000000341
H	-0.000000217	-0.000000465	-0.000000103
H	0.000000223	-0.000000147	-0.000000089
H	-0.000000035	-0.000000045	-0.000000042
H	-0.000000019	-0.000000065	0.000000115
H	-0.00000002	-0.000000069	-0.000000128
H	-0.000000055	-0.000000114	-0.000000171
H	-0.000000017	-0.000000088	-0.00000015
H	-0.000000191	0.000000087	0.000000077
H	-0.000000046	0.000000056	0.000000034
H	-0.000000171	0.000000011	-0.00000002
H	0.000000035	-0.000000079	0.00000014
H	0.000000026	-0.000000059	0.000000081
H	0.000000014	-0.000000038	0.00000011

Table S5: Cartesian coordinates of the S0 optimized geometry of the macrocycle **1⍰4H**$^{+}$ optimized at B3LYP/6-31G(d) level of theory

Sum of imaginary frequencies = 0

Total Energy (hartree) = -6254.452396 Hartrees

Optimized structure Coordinates:

Chemical symbol	Coordinates (Angstroms)		
	X	Y	Z
S	0.000000886	-0.00000099	-0.000001865
S	-0.000000622	-0.00000061	-0.000000404
S	0.000000701	-0.000001186	0.000001289
S	-0.00000134	-0.000001298	0.000002794
N	-0.000004182	0.000002566	-0.000001146
N	-0.000001756	-0.000006418	0.000002123
C	-0.000001018	0.000006377	-0.00000348
N	0.000001898	-0.000005188	-0.000003303
N	0.000004291	0.000002312	0.000000612
N	0.000002202	-0.000000508	-0.000002577
C	-0.000001713	-0.000002831	0.00000162
C	0.000002193	-0.000000437	0.000000515
C	-0.000003198	-0.000002297	0.000003169
C	0.000003607	0.000002207	0.000003218
C	0	-0.000000994	-0.000001914
C	0.000004329	-0.000006584	0.000001947
C	0.000003843	0.00000135	-0.000000589
C	0.00000359	0.00000055	-0.000003049
C	-0.00000599	0.000000876	0.000001849
C	-0.000000042	0.000006178	-0.00000333
C	-0.00000412	0.000002267	-0.000006057
C	-0.000005877	0.000001972	0.000001334
C	0.000006177	-0.00000413	-0.000000272
C	0.000003742	0.000003568	-0.000000239
C	0.000001203	-0.000000971	0.000001971
C	-0.000000979	-0.000006125	-0.000000476
C	0.000000481	0.00000101	0.000000355
C	-0.000002218	-0.000002147	-0.000000175
C	0.000002951	-0.000000912	-0.000001456
C	-0.000000441	0.000005068	-0.000001569
C	-0.000001915	-0.000001009	0.000000382
C	-0.000000146	-0.000000242	0.000001363
C	0.00000546	0.000001863	-0.000002646
C	-0.000000696	0.00000015	0.000001739
C	-0.000000007	0.000004933	-0.000000081
C	-0.000000936	-0.000005328	0.000000234
C	-0.000001307	0.000001364	0.000000095
C	0.00000024	-0.000000877	0.000001888
C	-0.000002022	-0.000002025	0.000001382
C	-0.000000041	0.000002034	-0.000000692
C	0.000001601	-0.000001278	-0.000000203
C	0.000001403	0.000004494	-0.000001449
C	0.000005108	-0.000000128	-0.000003339
C	0.000000188	-0.000004561	0.000000996
N	-0.000000639	-0.000001093	0.000008

C	0.000004655	-0.000003996	0.000004744
C	-0.000002097	-0.000000854	-0.000000687
C	0.000000022	0.000001043	0.000001003
C	0.000000385	-0.000000171	0.000000264
C	-0.000000148	0.000000538	-0.000000072
C	0.000002491	-0.000003287	-0.000002517
C	-0.00000052	0.000005373	-0.000000072
C	-0.000002635	-0.000002457	-0.000000401
C	-0.000001293	-0.000001437	0.000001847
C	-0.000007085	-0.000004074	-0.000000073
C	-0.000000695	0.000005367	0.000003196
C	-0.000001537	0.000004711	0.000001253
C	-0.000004278	0.00000145	0.000000894
C	-0.000004845	-0.000006524	-0.000001457
C	0.000000306	-0.000000243	-0.000001099
C	0.000007723	0.000001965	-0.000001168
C	-0.000005199	0.000003368	0.000000581
C	0.000000197	-0.000000763	-0.00000118
C	-0.00000022	0.000000009	0.000000684
C	0.000001796	-0.000001676	-0.000000796
C	-0.000000466	0.000000149	0.000000404
C	0.000000556	-0.000001204	-0.000002384
C	0.000000411	0.000000168	-0.000000584
C	0.000000216	0.000000048	-0.000001356
C	-0.000000616	-0.000000137	-0.000000327
C	0.000000397	0.000000471	0.00000036
C	-0.000000241	0.000000258	-0.000000532
C	0.000000506	0.000001956	0.000000999
C	0.000000188	0.000000975	-0.000000689
C	0.000000184	-0.000000402	0.00000009
C	0.000000529	-0.000000527	-0.000000265
C	-0.000000367	-0.000000113	-0.000001289
C	0.000000056	-0.000000382	0.000000774
C	-0.000000309	-0.000000216	0.000000116
C	0.00000008	-0.000004695	-0.000000083
C	-0.000000117	0.000000167	-0.000000276
C	0.000004476	0.000003919	-0.000002391
C	-0.000004903	-0.000000379	0.000004124
C	-0.00000011	-0.000000868	-0.00000065
C	0.000000145	0.000000385	0.000000192
C	-0.000000589	-0.000000513	0.000000211
C	0.000000323	0.000000216	0.000000103
C	0.000000345	0.000000068	0.00000045
C	-0.00000441	0.000001299	-0.000000036
C	0.000006861	0.000004809	0.000002546
C	0.000002803	-0.000002144	0.000000234
C	-0.000002957	-0.000000899	0.000000154
C	0.000000039	-0.000000114	0.000000566

C	0.000003506	-0.000002421	-0.000002577
C	0.000002394	-0.000001833	-0.000001217
C	0.000002141	0.000000539	0.000000829
C	-0.000000139	-0.0000006	-0.000000809
C	-0.000000193	-0.000000118	-0.000000572
C	0.000000474	-0.000000118	0.000001114
C	-0.000004449	-0.000003399	-0.000002645
C	0.000001245	0.000005763	0.00000114
C	0.000001011	0.000005681	0.000002118
C	-0.000001284	-0.000001492	0.000000682
C	-0.000007	0.000001183	0.000001316
C	-0.000006593	0.000004533	-0.000002263
C	0.000004043	0.000001085	0.000000147
C	0.000000548	0.000000528	-0.000000077
C	-0.000000001	-0.000000177	-0.000000486
C	-0.000000952	0.000000675	-0.000000198
C	-0.000000308	-0.000000298	0.000000036
C	0.000000602	-0.000000504	-0.00000068
C	-0.000000237	0.000000093	0.000000148
C	-0.000000236	0.000000375	-0.000000505
C	0.000000543	0.000000563	-0.000000232
C	-0.000000918	-0.000000307	0.000000065
C	0.000000164	0.000000351	0.000000077
C	-0.00000017	0.000000175	0.000000507
C	0.000000098	0.000000197	0.000000159
C	-0.000000446	0.000000429	0.000001175
C	0.000000175	0.000000238	-0.000000606
C	0.000000374	0.00000021	-0.000000073
C	0.000000244	-0.000000072	0.00000005
H	-0.000000267	-0.000000309	0.000000764
H	0.000000057	-0.000000298	-0.000000203
H	0.000000282	-0.000000655	-0.000000797
H	0.000000287	0.000000031	-0.000000408
H	0.000000076	-0.000000263	-0.000000587
H	-0.00000025	-0.000000047	-0.000000413
H	-0.00000072	0.000000525	0.000000249
H	-0.000000002	0.000000117	-0.000000245
H	0.000000179	0.000000155	0.000000538
H	0.00000019	-0.00000028	-0.000000304
H	0.000000506	0.000000209	0.000000086
H	-0.000000345	0.000000383	0.000000064
H	0.00000027	0.000000414	0.00000109
H	-0.000000226	0.000000047	-0.00000019
H	-0.000000292	0.000000408	0.000000843
H	0.000000258	-0.000000072	-0.000000066
H	0.000000064	-0.000000094	0.000000358
H	0.000000027	0.000000339	0.000000009
H	-0.000000039	0.000000114	0.000000222

H	0.000000005	0.000000104	-0.000000094
H	-0.000000114	-0.00000006	0.000000466
H	0.000000033	0.000000144	0.000000106
H	0.000000032	0.000000173	-0.00000009
H	-0.00000026	-0.000000079	0.000000052
H	-0.000000052	-0.000000028	-0.000000171
H	0.000000151	-0.000000031	0.000000301
H	-0.000000118	-0.000000141	0.000000107
H	-0.000000153	0.000000104	0.000000123
H	-0.000000121	0.000000152	0.000000068
H	-0.000000017	0.000000071	0.00000006
H	0.000000078	-0.000000032	0.000000101
H	0.000000621	-0.000000063	-0.000000298
H	0.000000275	-0.000000201	-0.000000114
H	0.000000116	0.000000095	-0.000000057
H	-0.000000408	-0.000000126	-0.000000262
H	-0.000000517	0.000000167	0.000000075
H	-0.000000063	0.000000025	0.000000042
H	0.000000164	0.000000238	0.000000358
H	0.000000042	0.00000027	-0.000000005
H	-0.000000105	-0.00000008	-0.000000344
H	-0.000000024	0.000000065	-0.000000074
H	0.000000066	-0.00000002	-0.00000023
H	0.000000093	-0.000000026	-0.000000052
H	0.0000001	0.000000144	-0.000000606
H	-0.00000004	0.00000007	0.000000045
H	0.000000233	-0.000000335	-0.000000361
H	-0.00000003	0.000000111	0.000000075
H	-0.000000016	0.00000006	-0.000000067
H	0.000000143	0.000000063	-0.00000013
H	0.000000085	0.000000135	-0.000000055
H	-0.000000124	-0.000000127	0.000000014
H	0.000000017	-0.000000011	0.000000108
H	-0.000000063	-0.000000173	0.000000253
H	0.000000044	0.000000191	0.000000189
H	0.000000484	-0.000000329	0.000000157
H	-0.00000197	-0.00000128	-0.000001611
H	-0.000000186	0.000000063	0.000000256
H	-0.000000054	-0.00000017	0.000000415
H	-0.000000186	-0.00000028	-0.000000366
H	-0.000000084	0.000000074	0.00000005
H	0.000000127	-0.000000122	0.000000225
H	0.000000371	0.000000162	-0.000000052
H	-0.000000062	-0.000000041	-0.000000122
H	-0.000000612	-0.000000055	0.00000022
H	-0.000000301	-0.000000161	0.000000072
H	0.000000225	0.000000358	-0.000000471
H	0.000000094	-0.000000126	0.000000011

H	0.00000025	0.000000282	-0.000000351
H	0.000001829	-0.000001431	0.000001304
H	-0.000000518	-0.000000467	-0.000000168
H	0.000000108	-0.000000005	-0.000000124
H	0.000000469	-0.000000957	-0.00000003
H	0.000000086	-0.000000015	0.000000214
H	-0.000000474	0.000000897	-0.00000038
H	0.000000149	-0.000000164	-0.000000108
H	0.000000186	-0.000000047	-0.000000056
H	0.000000099	-0.00000009	0.000000063
H	-0.000000424	0.000000809	0.000000082
H	0.000000932	-0.000000563	-0.000000195
H	0.000000038	-0.000000058	0.000000002
H	-0.000000837	-0.000000465	0.000000406
H	0.000000175	0.000000004	0.000000196
H	0.000000032	-0.000000018	0.000000164
H	0.000000819	0.000000545	-0.000000435
H	-0.000000318	-0.000000815	0.00000097
H	0.000000542	0.000000218	-0.00000067
H	-0.000000015	-0.000000168	0
H	0.000000103	-0.00000001	0.000000056
H	0.000000105	-0.000000048	-0.000000098
H	0.000000188	-0.000000577	-0.0000002
H	-0.000000284	0.000000225	0.000000248
H	-0.000000012	-0.000000063	-0.000000091
H	-0.000000418	0.000000148	0.000000155
H	-0.000000022	0.000000003	-0.000000082
H	0.000000273	-0.000000314	-0.000000328
H	-0.000000074	-0.000000146	0.000000011
H	0.000000064	-0.000000041	0.000000132
H	-0.000000144	-0.000000136	0.000000075
H	0.000000235	0.000000092	0.000000315
H	-0.000000058	-0.000000092	0.000000229
H	-0.000000121	-0.000000139	0.000000118
H	-0.000000077	-0.000000355	0.000000078
H	0.000000034	-0.000000013	-0.000000002
H	0.000000003	-0.000000112	0.0000001
H	-0.000000169	-0.000000006	-0.000000011
H	-0.000000342	-0.000000121	0.000000069
H	-0.000000803	0.000000117	0.000000241
H	-0.000000059	0.000000527	-0.000000885
H	0.000000245	0.000000576	-0.000001678
H	0.000000655	0.000000438	0.000000749

9. Supporting References

[S1] Gaussian 16, Revision C.01, Frisch MJ, Trucks GW, Schlegel HB, Scuseria GE, Robb MA, Cheeseman JR, Scalmani G, Barone V, Petersson GA, NakatsujiH, Li X, Caricato M, Marenich AV, Bloino J, Janesko BG, Gomperts R, Mennucci B, Hratchian HP, Ortiz JV, Izmaylov AF, Sonnenberg JL, Williams-Young D, Ding F, Lipparini F, Egidi F, Goings J, Peng B, Petrone A, Henderson T, Ranasinghe D, Zakrzewski VG, Gao J, Rega N, Zheng G, Liang W, Hada M, Ehara M, Toyota K, Fukuda R, Hasegawa J, Ishida M, Nakajima T, Honda Y, Kitao O, Nakai H, Vreven T, Throssell K, Montgomery JA Jr, Peralta JE, Ogliaro F, Bearpark M, Heyd JJ, Brothers EN, Kudin KN, Staroverov VN, Keith T, Kobayashi R, Normand J, Raghavachari K, Rendell A, Burant JC, Iyengar SS, Tomasi J, Cossi M, Millam J M, Klene M, Adamo C, Cammi R, Ochterski JW, Martin RL, Morokuma K, Farkas O, Foresman JB, Fox DJ. Gaussian, Inc., Wallingford CT, 2016.

[S2] (a) A. D. Becke, *J. Chem. Phys.,* **1993**, *98*, 1372; (b) C. Lee, W. Yang and R. G. Parr, *Phys. Rev. B*, **1988**, *37*, 785.

[S3] (a) R. Bauernschmitt, R. Ahlrichs, *Chem. Phys. Lett.* **1996**, *256*, 454-464; (b) R. E. Stratmann, G. E. Scuseria, M. J. Frisch, *J. Chem. Phys.* **1998**, *109*, 8218-8224; (c) M. E. Casida, C. Jamorski, K. C. Casida, D. R. Salahub, *J. Chem. Phys.* **1998**, *108*, 4439-4449.

[S4] (a) A. Kalaiselvan, I. S. Vamsi Krishna, A. P. Nambiar, A. Edwin, V. S. Reddy, S. Gokulnath, *Org. Lett*. **2020**, *22*, 4494–4499. (b) Naniyil, A.; Koroth Valappil, N.; Andrews, A. P.; Gokulnath, S. *Chem. Commun*. **2024**, *60*, 6957–6960.